THE EUROPEAN
PHYSICAL JOURNAL C

A coupled-fluid approach to explore bounce and inflationary cosmology with Barrow holographic as the driving dark fluid

Sanghati Saha[1,a] , **Surajit Chattopadhyay**[1,b] , **Ertan Güdekli**[2,c]

[1] Department of Mathematics, Amity University, Kolkata, Major Arterial Road, Action Area II, Rajarhat, New Town, Kolkata 700135, India
[2] Department of Physics, Istanbul University, Istanbul 34134, Turkey

Abstract Assuming that viscous fluid in the form of Barrow holographic dark energy (BHDE) (a particular case of more generalized version of HDE elaborated in Nojiri et al. in Phys Lett B 825:136844, 2022; Symmetry 13(6):928, 2021) and pressure-less dark matter are present across the flat Friedmann–Robertson–Walker universe, we find the precise solutions of viscous BHDE models in non-interacting and interacting scenarios for different choices of scale factor. We show the evolution of the EoS parameters in the viscous non-interacting and interacting situations together with the deceleration parameters for observing the transition time frame. Afterwards, we investigate a bounce inflation model using the analytical results of model's slow-roll parameters, scalar spectral index, and tensor-to-scalar ratio. We investigated an association between BHDE and scalar field models since inflation is typically attributed to the existence of scalar fields. The evolution of the generated potential from the scalar fields are plotted against time. Finally, we investigated the GSL of the thermodynamics.

1 Introduction

The accelerating expansion of the universe has been widely proven by cosmological evaluations obtained with the Supernovae Ia (SNeIa), the Cosmic Microwave Background (CMB) radiation anisotropy, the Large Scale Structure (LSS), and X-ray investigations [1–13]. Most scientists believe that this accelerating expansion is caused by an energy component, commonly known as Dark Energy (DE) with nega-

[a] e-mails: sanghati.saha1504@gmail.com;
sanghati.saha2@s.amity.edu

[b] e-mails: schattopadhyay1@kol.amity.edu;
surajitchatto@outlook.com (corresponding author)

[c] e-mail: gudekli@istanbul.edu.tr

tive pressure. Recent cosmological observations show that the DE occupies roughly two-thirds of the universe's total density while DM fills the remaining one-third (baryonic matter makes up only a small percentage of the universe's overall energy density) [14,15]. Radiation barely makes an impact in universe's evolution. Numerous candidates have been proposed to define DE [16–19], but its nature is still undetermined. The simplest form of DE is cosmological constant with a negative constant equation of state (EoS) parameter $\omega = -1$ [20,21]. There have been numerous other dark energy models proposed, including quintessence [22–24], phantom [25–28], quintom [29–32], tachyon field [33–35], k-essence [36–38], Chaplygin gas [39–42], holographic dark energy [43–45], and many more to explain the accelerated expansion of the universe. For an extensive review on dark energy we can study this paper [46]. The holographic dark energy (HDE), whose formulation depends on the holographic principle [47], is a further candidate for DE. According to the holographic principle, which derives from black hole (BH) thermodynamics, a system's entropy is determined by its area rather than its volume [48,49]. The realisation that information on every object that has entered a black hole (BH) is encoded on the surface of the event horizon served as the inspiration for the concept. Susskind expanded the holographic idea to include string theory in [48]. Additionally, he recently developed the de-Sitter space holography in [50]. Starting with the relationship between a quantum field theory's greatest length and its ultraviolet cutoff [51], one may arrive at a vacuum energy of holographic origin that, at cosmic scales, takes the form of dark energy. Both in its simplified [52–55] and expanded [56–65] forms, holographic dark energy produces intriguing cosmic behaviour that is consistent with observational data [2,66–71].

The Bekenstein–Hawking entropy of a black hole is equivalent to the universe horizon (i.e., maximum distance) entropy, which is proportional to its area in the application of

the holographic principle at cosmic framework. However, Barrow recently showed that more intricate, fractal characteristics might be introduced to the black-hole structure via quantum gravity forces, which were motivated by the COVID-19 viral images. Due to this complicated structure's finite volume but with indefinite (or finite) area, the deformed black-hole entropy formula [72] is

$$S_h = \left(\frac{A}{A_0} \right)^{1+\frac{\Delta}{2}} \qquad (1)$$

where, A denotes usual horizon area and A_0 denotes Planck area. The new exponent Δ is used to measure the quantum-gravitational deformation, with $\Delta = 0$ denoting the conventional Bekenstein–Hawking entropy (horizon structure) and $\Delta = 1$ denoting the most complex and fractal structure. Though it resembles Tsallis non-extensive entropy [73], the above quantum-gravitationally corrected entropy differs from the typical "quantum-corrected" entropy with logarithmic adjustments [74].Yet, basic fundamentals and physical concepts are very different. The fact that the aforementioned effective fractal behaviour derives from wide elementary physical principles rather than from precise quantum gravity calculations, making it appropriate as a starting approach [72] to the subject.

In modern theoretical cosmology, one of the most fundamental concern is whether the universe was singular or non-singular at its beginning. Asking whether the Big Bang or Big Bounce theories accurately capture the evolution of our universe is analogous to this question. In the bouncing model, the Universe first experiences a contraction phase that is dominated by matter, followed by a non-singular bounce, before causal production for fluctuation [75–78]. Additionally, the scale factor grows ($a(t) > 0$) during the expanding phase and lowers ($a(t) < 0$) during the contracting phase. Finally, at the matter bounce epoch, the scale factor is equal to zero. As a result, in bouncing cosmic theory, the Hubble parameter H transitions from negative values $H < 0$ to positive values $H > 0$ by crossing zero ($H = 0$) [79,80]. One of the another potential explanations for the early universe's development is inflation, according to scientific literature. According to this, the universe expands at an extremely rapid pace and in a short period of time. Starobinsky [81] offered such an expansion theory for the early ages, and Guth [82] used it for the first time as a potential fix for the hot big-bang theory's issues. This inflationary scenario has been thoroughly investigated and generalised in several ways [83–88] which are consistent with observational data. Although, conventional inflation scenario still requires improvement due to the so-called "singularity problem" that Hawking et al. presented in their landmark paper on the singularity theorem [89–91]. Their proof of this theorem states that, if inflation is traced back to its inception, we are likely to come across the Big-Bang singu-

larity, which is the singularity of the early the universe. At the singularity, everything blows up and one can not get control of the universe under classical description. Since the singularity occurs before the onset of inflation, it can hardly be solved within inflation scenario itself. This motivates us to find alternative theories in pre-inflation era. In order to get rid of this problem we have considered bouncing evolution of the universe. It is also possible to extend this non-singular scenario to the cyclic universe [92–95] in a significant way. The concept, which we shall refer to as the bouncing inflation model for convenience, has been investigated in Refs. [96,97]. In this model, the universe is in a contracting phase before to the slow-roll inflation [98–103] and begins to inflate after the bounce. The contracting phase of this model is comparable to that of the Pre-BigBang scenario (reviews can be found in [104,105]) (PBB scenario), and it may also be comparable in theory to the ekpyrotic scenario. Contrary to the findings, the adiabatic perturbation spectrum produced during the kinetic contraction in the PBB scenario is very blue. On large angular scales, however, this blue spectrum is only necessary for the power suppression [96]. The reheating temperature must be appropriate with a hot big bang evolution after inflation, and the slow-roll inflation must typically begin at a high scale. These requirements ensure that the magnitude of primordial perturbation is compatible with the observations. The application of the holographic principle to the early universe will yield an energy density that is great enough to sustain the inflationary scenario, as the measure of length during the inflationary period is anticipated to be tiny. According to a recent argument, the start of the slow-roll inflation will need an enormous uptunneling in the everlasting inflation scenario, which is exponentially unfavourable, if the magnitude of the eternally inflating backdrop is extremely low. Nevertheless, this outcome might be considerably changed if the bounce was introduced prior to the slow-roll inflation (see [106–109,113–116]). It is demonstrated in Ref. [107] that the universe may be at various minimums of a landscape at different cycles, and that the development of the observed universe is explained by the bouncing inflation model. The inflation after bounce results in cosmological hysteresis, which raises the amplitude of the cycles, as demonstrated in Ref. [109]. The early-time acceleration and late-time acceleration eras of our universe were unifiedly described by Nojiri et al. [110] using the holographic technique. It was discovered that several greater curvature cosmological models, with or without matter fields, corresponded to this "holographic unification." Both inflation and bounce realizations in holographic framework were proposed in [111,112].

Cosmic expansion is significantly influenced by dissipate processes, such as heat transmission, shear viscosity, and bulk viscosity. Eckart [117] first presented the general theory of dissipation in a relativistic imperfect fluid, which Landau and Lifshitz [118] later refined. A relativistic second-order the-

ory known as the full causal theory was created by Israel and Stewart [119]. Shear viscosity refers to an an-isotropic universe, whereas bulk viscous pressure is connected to dissipate events in an uniform homogeneous and isotropic universe. When a cosmic fluid expands (or shrinks) too quickly, the system may not have enough time to reach its local thermodynamic equilibrium, leading to the formation of bulk viscosity.

Bekenstein [120] made the assumption in 1973 that there is a correlation between a black hole's event horizon and its thermodynamics, such that the event horizon of the black hole is a measure of its entropy. This concept has been extended to include the horizons of cosmological models, and now each horizon relates to an entropy. In generalised form, the second law of thermodynamics has been modified in this way: the total of all time derivatives of entropy(s) associated to horizons plus the time derivative corresponding to normal entropy has to be positive, i.e., the total amount of entropy(s) must be increasing as a function of time. In [121], it is examined if the generalised second law (GSL) holds true for cosmological models that somewhat deviate from de-Sitter space. As the horizon area quantifies our lack of comprehension of what is beyond it, it is only reasonable to connect an entropy with it.

Thus, whether theoretically or observationally, studying the bouncing inflation model is interesting. We look over the fundamental BHDE equations in Sect. 2. In Sect. 3 we have introduced the scale factors and established the dynamics of cosmological parameters corresponding to the scale factors in viscous interacting and non-interacting scenario. In Sect. 4 we have discussed in detail about the inflationary scenario with focus on non-singular bounce inflation. In Sect. 5, we also explore the thermodynamic properties of this present model. Section 6, finally the paper ends with some conclusions and future directions. It may be noted that in the figures, the unit of time is Gyears. The model parameters and the constants of integration present in the equations are dimensionless and hence no unit is used for them. This holds for the previous and subsequent discussions.

Rest of the paper is organized as follows: In Sect. 2, we have presented a discussion on BHDE in the framework of bulk viscosity. Bouncing cosmology incorporating dark energy-dark matter interaction has been demonstrated in Sect. 3. Barrow holographic dark fluid-driven inflation is discussed in Sect. 4. GSL implications of BHDE are discussed in Sect. 5 and the work is concluded in Sect. 6.

2 An overview of Barrow holographic dark energy in bulk viscous framework

In this section, we consider Barrow holographic dark energy (BHDE) in bulk viscous scenario. Considering the entropy

condition $S \propto A \propto L^2$ with usual entropy relation $\rho_{DE} L^4 \leq S$ where, ρ_{DE} defines standard holographic dark energy and L defines length of the horizon. By using black-hole entropy formula Eq. (1) we can derive energy density of Barrow Holographic Dark Energy(BHDE) as following

$$\rho_{DE} = cL^{\Delta-2} \tag{2}$$

Here, $c = 3p^2 M_p^2$, in which M_p denotes reduced Planck mass, p^2 is our model parameter, Δ denotes quantum gravitational deformation, and L is the length of IR cut-off. The aforementioned estimation gives the predicted standard holographic dark energy in the scenario when $\Delta = 0$. However, Barrow holographic dark energy will diverge from the conventional one by changing the range of Δ, resulting in distinct cosmic behaviour. Although there are other options for the greatest length L that occurs in the expression of any holographic dark energy, the future event horizon is the one that is most frequently used in the literature [122,123].

$$R_E = a \int_t^\infty \frac{dt}{a} = a \int_a^\infty \frac{da}{Ha^2} \tag{3}$$

where, a denotes scale factor and $H = \frac{\dot{a}}{a}$ be the Hubble parameter. As a result, by replacing L in equation Eq. (2) with R_E, we get to the energy density of BHDE, which is

$$\rho_{BHDE} = cR_E^{\Delta-2} \tag{4}$$

In this case, we have considered the range of $\Delta > 0$ and $M_p^2 = 1$. Therefore, in Eq. (4) the term c behaves like our model parameter. For a homogeneous and isotropic flat universe, the FRW metric is provided by

$$ds^2 = -dt^2 + a^2(t)(dr2 + r^2(d\theta^2 + sin^2\theta d\phi^2)), \tag{5}$$

where, the cosmic time is represented by t, and the scale factor is $a(t)$. Here, we have take in the units $8\pi G = 1$. Any dissipation process in a FRW cosmology is scalar in the case of isotropic and homogeneous cosmologies. The potential for DEC violations is a well-known outcome of the FRW cosmological solutions, which correspond to universes with perfect fluid and bulk viscous stresses [124,125]. The bulk viscous pressure Π in Eckart's theory [117] can be chosen as $\Pi = -3H\xi$ where ξ is the term describing the fluid's bulk viscosity and may be defined as a function of the Hubble parameter due to transport coefficient. We see that in [126] $\xi \propto \rho$ and $\rho \propto H$. Additionally, Meng and Dou [127] presume the bulk viscosity coefficient in terms of Hubble parameter H. Based on the aforementioned studies, we have taken into consideration $\xi(H) = \xi H$ in this study, where ξ is a constant parameter. Therefore, the resulting model interprets the universe's bulk viscous pressure as $\Pi = -3\xi H^2$. We assume that the universe contains both the aforementioned Barrow holographic dark energy and ordinary matter perfect fluid in bulk viscous scenario. Following that, the two

Friedmann equations are expressed as

$$H^2 = \frac{1}{3}\rho_{effective} \tag{6}$$

and,

$$6\frac{\ddot{a}}{a} = -(\rho_{effective} + 3(P_{effective} + \Pi)) \tag{7}$$

where, $\rho_{effective} = \rho_m + \rho_{BHDE}$. Here, we have considered, pressure-less dark matter whose density is denoted by ρ_m and $P_m = 0$. The effective pressure, P_{eff}, is just redefined by the bulk viscosity, causing dissipation, according to $P_{effective} = P_{BHDE} = P_{DE} + \Pi = P_{DE} - 3\xi H^2$.

3 The bouncing cosmology incorporating dark energy and dark matter interaction

The most interesting aspect of the cosmic bounces, compared to the conventional inflationary paradigm, is the lack of the initial singularity. A successful bouncing cosmology should, in theory, overcome every issue that the inflationary scenario resolved. It should also result in the production of a power spectrum that is almost scale invariant. There are many inflationary bouncing cosmologies in the literatures [128–130], and in this section, before mentioning the details of challenges of early universe cosmology in the Big Bang cosmology era as well as bouncing scenarios to address some of the conceptual problems such as inflation, horizon, and entropy, we must begin with a lightning of physical properties of the scale factors. We shall here check the mixed model as BHDE background fluid, in which a contracting phase followed by a bounce leads to an inflationary era.

3.1 Scale factors chosen

In this section, we are going to explore emergent, intermediate scale factors in the viscous BHDE, Big-Bang cosmological settings.

3.1.1 Emergent expansion of the universe

The scale factor for emergent universe [131,132] can be determined as

$$a(t) = a_0(\lambda + e^{\mu t})^n \tag{8}$$

in which, a_0, μ, λ, n being positive invariant. In order for the scale factor $a(t)$ to be positive and $a_0 > 0$ must be met and for avoidance of big-rip singularity λ has to be positive respectively. For accelerated expansion of the universe the scale factor $a(t)$ must be positive, as well as n has to be positive. To achieve big-bang singularity at $t = -\infty$ we have to take, $a < 0$ and $n < 0$. Therefore, we can derive

Hubble parameter (H) from Eq. (8) which are:

$$H = \frac{n\mu e^{\mu t}}{(\lambda + e^{\mu t})} \tag{9}$$

3.1.2 Intermediate expansion of the universe

Considering a specific kind of intermediate scenario where the Friedmann universe's scale factor $a(t)$ [133,134] is defined as;

$$a(t) = e^{Bt^\beta} \tag{10}$$

where, β, B are positive constant and β lies between (0, 1). Here, the universe is expanding more quickly compared to the power law form, where the scale factor is stated as, ($a(t) = a_0 t^n$, n be the constant) as well as the expansion of the universe is slower than de-sitter expansion rate with $\beta = 1$. Therefore, Hubble parameter becomes

$$H = B\beta t^{\beta-1} \tag{11}$$

3.2 Bouncing universe

In this matter bounce scenario, the initial singularity seen in both the inflationary and standard Big Bang cosmologies may be properly avoided. In the bouncing model, the Universe first experiences a contraction phase that is dominated by matter, followed by a non-singular bounce, before causal production for fluctuation [75–78]. Additionally, the scale factor grows ($a(t) > 0$) during the expanding phase and lowers ($a(t) < 0$) during the contracting phase. Finally, at the matter bounce epoch, the scale factor is equal to zero. As a result, in bouncing cosmic theory, the Hubble parameter H transitions from negative values $H < 0$ to positive values $H > 0$ by crossing zero ($H = 0$) [79,80]. In this framework of BHDE, our goal with this article is to offer the latest developments in the discussion of the inflationary epoch, dark energy, as well as bouncing cosmology. Let us consider, a bouncing scale factor of double exponential form [135]
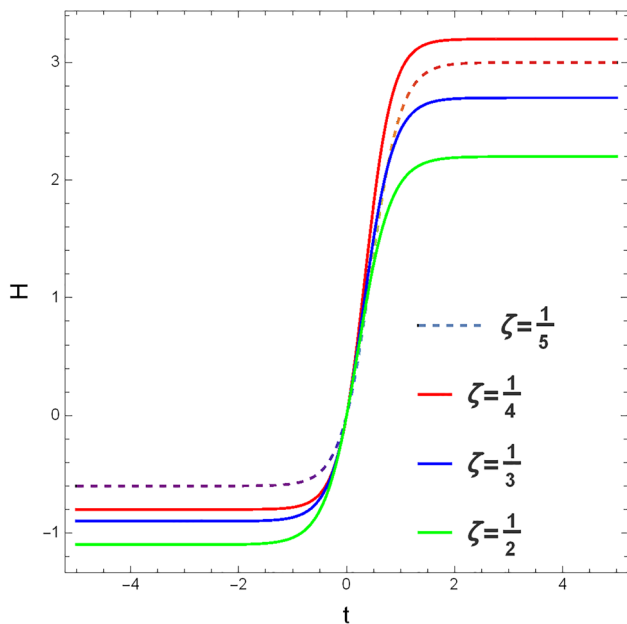
$$a(t) = a_0 e^{\mu t} + a_1 e^{-\gamma t} \tag{12}$$

where, a_0, a_1, μ and γ are positive real numbers. There will be de-sitter universe formed if $a_1 = 0$ and $\gamma = 0$ and for that reason we are assuming $a_1 \neq 0$ and $\gamma \neq 0$. Therefore,

$$\dot{a}(t) = a_0\mu e^{\mu t} - a_1\gamma e^{-\gamma t} \tag{13}$$

Therefore, the bouncing time will be

$$t_s = \frac{1}{\mu + \gamma}\log\left(\frac{a_1\gamma}{a_0\mu}\right)$$

Fig. 1 Evolution of bouncing Hubble parameter

In this case, we are taking non-singular bounce with bouncing point at $t = 0$ with the constraint $\frac{a_0}{a_1} = \frac{\gamma}{\mu} = \zeta$.

$$H = \frac{a_0 e^{t(\mu+\nu)}\mu - a_1\nu}{a_1 + a_0 e^{t(\mu+\nu)}} \quad (14)$$

In Fig. 1 we have shown evolution of Hubble parameter with respect to cosmic time. Here, we can see H is negative in pre-bounce scenario which shows contraction of the universe, $H = 0$ at bouncing point and $H > 0$ in post-bounce scenario by showing expansion of the universe.

3.3 Emergent cosmologies: general characteristics

Here, we have considered the density of BHDE from Eq. (4) where, Δ lies between $(0, 1)$ and c be the model parameter in the scenario of emergent universe from Eq. (8). Again, $\dot{R}_E$ can be calculated using Eq. (3) as $\dot{R}_E = HR_E - 1$ and solving it with the help of Eq. (9) we can get the solutions of R_E and which is

$$R_E = \left(e^{t\mu} + \lambda\right)^n C_1 + \frac{\left(1 + e^{-t\mu}\lambda\right)^n {}_2F_1\left[n, n; 1 + n; -e^{-t\mu}\lambda\right]}{n\mu} \quad (15)$$

Therefore, reconstructed energy density of BHDE in emergent scenario be:

$$\rho_{BHDE} = c\left(C_1\left(e^{t\mu} + \lambda\right)^n + \frac{\left(1 + e^{-t\mu}\lambda\right)^n {}_2F_1\left[n, n; 1 + n; -e^{-t\mu}\lambda\right]}{n\mu}\right)^{-2+\Delta} \quad (16)$$

3.3.1 Emergent BHDE universe: single fluid model

Here, we have considered non-interacting scenario for this case. Therefore, BHDE doesn't interact with the viscous stuff in its entirety. As a result, each of these fluids' continuity equations is conserved separately:

$$\dot{\rho}_m + 3H(P_m + \rho_m) = 0 \quad (17)$$

and,

$$\dot{\rho}_{Total} + 3H(\rho_{Total} + P_{Total}) = 0 \quad (18)$$

where, $\rho_{Total} = \rho_m + \rho_{BHDE}$ and, $P_{Total} = P_m + P_{DE} + \Pi$. As we have taken, pressure-less dark matter, $P_m = 0$ and therefore, $P_{Total} = P_{BHDE} - 3\xi H^2$. From Eq. (17), we got the solutions of matter density

$$\rho_m = \frac{\rho_{m_0}\left(e^{t\mu} + \lambda\right)^{-3n}}{a_0^3} \quad (19)$$

From Eqs. (16) and (19), we can get the solutions of ρ_{Total} and $\dot{\rho}_{Total}$.

$$\rho_{Total} = \frac{\rho_{m_0}\left(e^{t\mu} + \lambda\right)^{-3n}}{a_0^3} + c\left(C_1\left(e^{t\mu} + \lambda\right)^n + \frac{\left(1 + e^{-t\mu}\lambda\right)^n {}_2F_1\left[n, n; 1 + n; -e^{-t\mu}\lambda\right]}{n\mu}\right)^{-2+\Delta} \quad (20)$$

From Eq. (7) we can get the expression of thermodynamic pressure (P) and from Eqs. (18), (19) and (20) we can get the expression of EoS parameter w and we know that, effective EoS parameter w_{eff},

$$w_{eff} = \frac{P + \Pi}{\rho_{Total}} = \frac{\eta_1}{\eta_2} \text{ (Let)}, \quad (21)$$

where,

$$\eta_1 = -\rho_{m_0}\left(e^{t\mu} + \lambda\right)^{2-3n} - 9a_0^3 e^{2t\mu} n^2\mu^2\xi$$
$$+ a_0^3\left(6e^{2t\mu}n\mu^2 - 6e^{2t\mu}n^2\mu^2 - 6e^{t\mu}n\left(e^{t\mu} + \lambda\right)\mu^2\right.$$
$$+ 9e^{2t\mu}n^2\mu^2\xi - c\left(e^{t\mu} + \lambda\right)^2\left(C_1\left(e^{t\mu} + \lambda\right)^n\right.$$
$$\left.\left. + \frac{\left(1 + e^{-t\mu}\lambda\right)^n {}_2F_1\left[n, n; 1 + n; -e^{-t\mu}\lambda\right]}{n\mu}\right)^{-2+\Delta}\right)$$

$$\eta_2 = 3a_0^3\left(e^{t\mu} + \lambda\right)^2\left(\frac{\rho_{m_0}\left(e^{t\mu} + \lambda\right)^{-3n}}{a_0^3}\right.$$
$$\left. + c\left(C_1\left(e^{t\mu} + \lambda\right)^n + \frac{\left(1 + e^{-t\mu}\lambda\right)^n {}_2F_1\left[n, n; 1 + n; -e^{-t\mu}\lambda\right]}{n\mu}\right)^{-2+\Delta}\right)$$

We have now examined the stability of our model to see whether or not it adequately captures the expanding the universe. The Hubble parameter $H(t)$ explains how the universe's expansion is time-dependent although the expansion
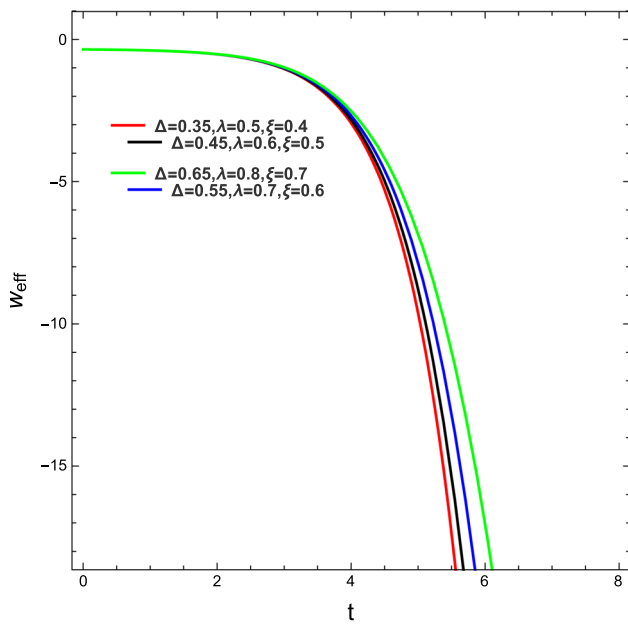
Fig. 2 Evolution of reconstructed effective EoS parameter of viscous BHDE in non-interacting emergent scenario
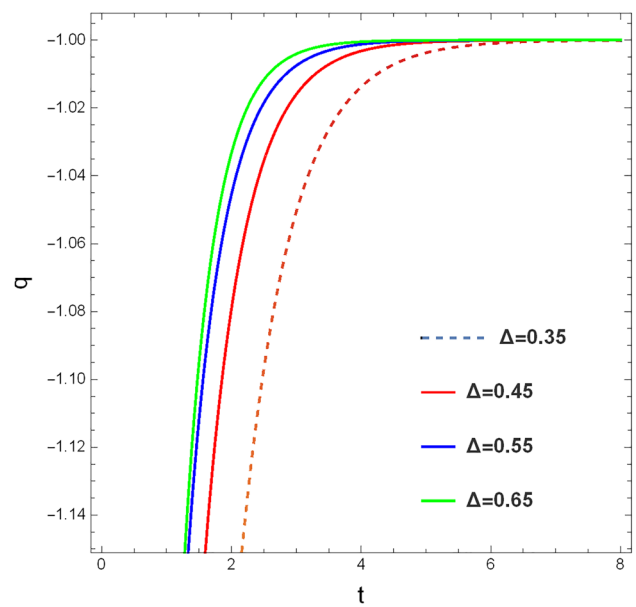

Fig. 3 Evolution of deceleration parameter in non-interacting emergent scenario

rate's variation over time is quantified by the deceleration parameter, $q(t)$ [136,137]. In this case, we established square speed of sound [138,139] to determine the model's stability. $c_s^2 \geq 0$ is necessary for the model's stability. A value below zero indicates that the model is unstable. Here, we used Einstein's theory of viscous non-interacting emergent behaviour and included the squared speed of sound for BHDE reconstruction scheme. The deceleration parameter ($q(t)$) and square speed of sound (c_s^2) are given by:

$$q(t) = \frac{-\ddot{a}(t)}{aH^2} \tag{22}$$

$$c_s^2 = \frac{d(P_{effective})}{d(\rho_{Total})} \tag{23}$$

where, $P_{effective} = P_{Total} = P_{BHDE} - 3\xi H^2$ and $\rho_{Total} = \rho_m + \rho_{BHDE}$ and $a(t)$ be the emergent scale factor.

In Figs. 2, 3 and 4 we have plotted w_{eff}, deceleration parameter (q) and c_s^2 with respect to cosmic time t for a range of values of Δ. We used the parameters as follows to create the diagrams for the current section: $c = 3$, $\rho_{m_0} = 0.32$, $C_1 = 2.6$, $\mu = 1.3$, $\lambda = 0.6$, $n = 0.06$, and $a_0 = 0.2$. All the choices are in their physically permissible ranges. It is observed that during the cosmological evolution, the reconstructed BHDE effective EoS parameter Fig. 2 behaves like phantom in viscous non-interacting emergent Einstein gravity framework. The deceleration parameter's value in Fig. 3 is precisely less than zero, demonstrating the universe's acceleration. The graph Fig. 4 shows that the model is stable for all values of Δ and ξ as long as the squared speed of sound is positive throughout its entire existence in a Friedmann–Lemaître–Robertson–Walker universe.
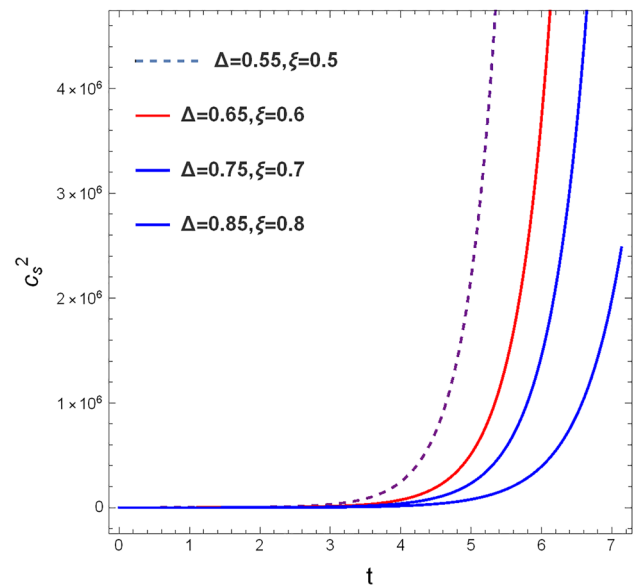
Fig. 4 Square speed of sound $c_s^2 \geq 0$ for viscous BHDE in non-interacting emergent scenario

3.3.2 Emergent BHDE universe: coupled fluid model

In this section, we suppose that the dark fluids of the universe-BHDE and pressure-less DM-exchange energy via an interaction term called Q. Therefore, the combined form of the conservation equations be:

$$\dot{\rho}_m + 3H\rho_m = Q \tag{24}$$

$$\dot{\rho}_{BHDE} + 3H\rho_{BHDE}(1 + w) = -Q \tag{25}$$

where, w be the EoS parameter. In the aforementioned equations, Q stands for the pace of energy density transfer. If $Q > 0$, energy transfer occurs from $BHDE \rightarrow DM$; if $Q < 0$, energy transfer occurs from $DM \rightarrow BHDE$. As a result, once the development of the energy densities ρ_m and ρ_{DE} is established for a certain interaction term Q, either numerically or analytically, the rate of expansion of the universe can be determined and the revised cosmological parameters may be explained in terms of their evolution through time. The interaction among BHDE and DM has to be a function of the densities of energy multiplied by a number with units of an inverse of time, a natural choice of Hubble parameter, according to the conservation of energy Eqs. (24) and (25). As a consequence, Q might be represented intuitively in any arbitrary way; for instance, $Q \propto H\rho$ with assumptions of $\rho = \rho_m$, $\rho = \rho_{DE}$, and $\rho = \rho_m + \rho_{DE}$ are more frequent in this context. In this present work, we have assumed $Q = 3Hb^2\rho_m$ from the literature [140]. Now, from Eq. (24), we can get the expression of ρ_m

$$\rho_m = \left(e^{t\mu} + \lambda\right)^{3(-1+b^2)n} C_2. \tag{26}$$

Therefore, from Eqs. (16) and (26), we can get the expression of ρ_{Total} and $\dot{\rho}_{Total}$ and by putting the value of ρ_{Total} and $\dot{\rho}_{Total}$ in Eq. (25) we got the expression of EoS parameter w in interacting viscous scenario and plotted in Fig. 5 with respect to time. Again, by putting the expression of ρ_{Total} and Π in Eq. (7) we got the expression of pressure (P) and we have plotted $w_{eff} = \frac{P + \pi}{\rho_{Total}}$ in interacting viscous scenario in Fig. 6. Here, we have checked the stability of the model in interacting scenario which is stable under small perturbations by getting $c_s^2 \geq 0$. The interacting EoS parameter w in Fig. 5 has been found to breach the -1 phantom border in the early stages of time. Then, it can avoid big-rip singularity in the later phase time and behaves like quintessence. In Fig. 6 the interacting effective EoS parameter behaves like phantom although the reconstructed interacting effective EoS parameter can not avoid the big-rip by exiting the phantom boundary.

### 3.4 Intermediate cosmologies: general characteristics

Here, we have considered, intermediate scale factor $a(t)$ from Eq. (10) by choosing β, B as positive arbitrary constant and β will be in $(0, 1)$. Again, the density of BHDE as

$$\rho_{BHDE} = cR_E^{\Delta-2}$$

where, Δ belongs to $(0, 1)$ and c be the model parameter. By solving R_E from $\dot{R}_E = HR_E - 1$ with the help of Eq. (11), we can get the expression of ρ_{BHDE} in intermediate scenario.
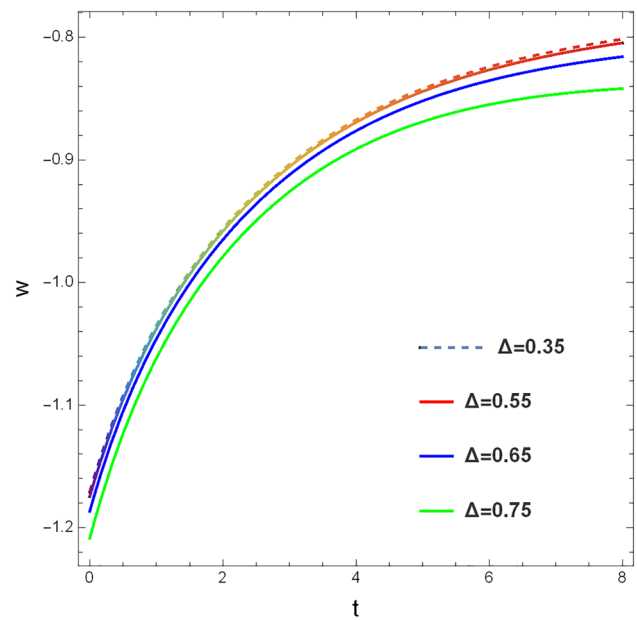
Fig. 5 Evolution of reconstructed viscous interacting EoS parameter with the range of interaction coefficient b lies in $(0, 1)$ in emergent scenario
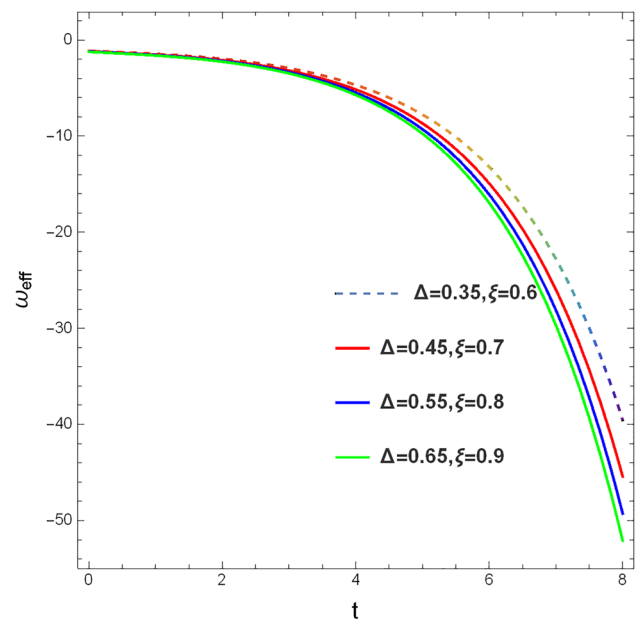
Fig. 6 Evolution of reconstructed viscous interacting effective EoS parameter with the range of interaction coefficient b lies in $(0, 1)$ in emergent scenario

Therefore,

$$R_E = e^{Bt^\beta}\left(C_1 + \frac{t\left(Bt^\beta\right)^{-1/\beta}\Gamma\left[\frac{1}{\beta}, Bt^\beta\right]}{\beta}\right) \tag{27}$$

and,

$$\rho_{BHDE} = c \left(e^{Bt^\beta} \left(C_1 + \frac{t \left(Bt^\beta \right)^{-1/\beta} \Gamma\left[\frac{1}{\beta}, Bt^\beta\right]}{\beta} \right) \right)^{-2+\Delta}.$$

(28)

3.4.1 Intermediate BHDE universe: single fluid model

In this subsection, we have considered intermediate non-interacting scenario. Therefore, from Eq. (17), we can get the density of pressure-less dark matter,

$$\rho_m = \rho_{m_0} e^{-3Bt^\beta}$$

(29)

Therefore, from Eqs. (28) and (29) we can get the expression of ρ_{Total} which is

$$\rho_{Total} = c \left(e^{Bt^\beta} \left(C_1 + \frac{t \left(Bt^\beta \right)^{-1/\beta} \Gamma\left[\frac{1}{\beta}, Bt^\beta\right]}{\beta} \right) \right)^{-2+\Delta}$$
$$+ \rho_{m_0} e^{-3Bt^\beta}$$

(30)

Therefore, from Eq. (7), the expression of thermodynamic pressure of BHDE.Therefore, the expression of EoS parameter be,
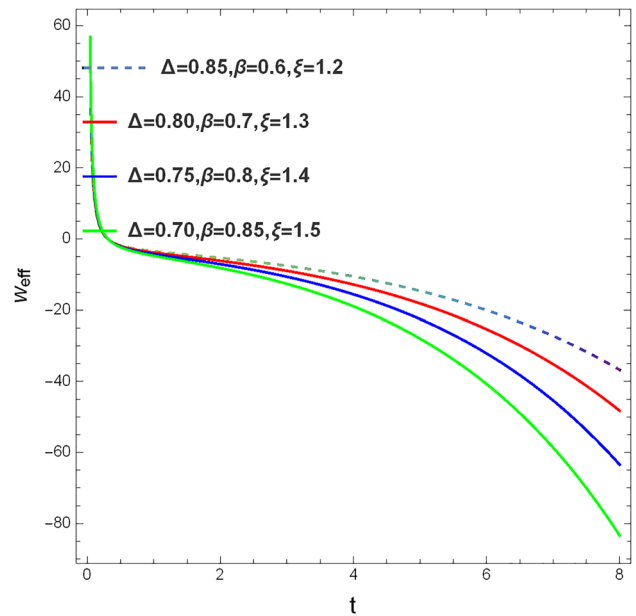
$$w = \frac{\zeta 11}{\zeta 22}$$

(31)

where,

$$\zeta 11 = -c t^{-\beta} \left(Bt^\beta \right)^{2/\beta} \beta^2$$
$$\times \left(e^{Bt^\beta} \left(C_1 + \frac{t \left(Bt^\beta \right)^{-1/\beta} \Gamma\left[\frac{1}{\beta}, Bt^\beta\right]}{\beta} \right) \right)^\Delta$$
$$\times \left(2t \left(Bt^\beta \right)^{\frac{1}{\beta}} + BC_1 e^{Bt^\beta} t^\beta \left(Bt^\beta \right)^{\frac{1}{\beta}} \beta - t \left(Bt^\beta \right)^{\frac{1}{\beta}} \Delta \right.$$
$$+ BC_1 e^{Bt^\beta} t^\beta \left(Bt^\beta \right)^{\frac{1}{\beta}} \beta \Delta$$
$$+ B e^{Bt^\beta} t^{1+\beta} \Gamma\left[\frac{1}{\beta}, Bt^\beta\right]$$
$$\left. + B e^{Bt^\beta} t^{1+\beta} \Delta \Gamma\left[\frac{1}{\beta}, Bt^\beta\right]^{gg} \right)$$

and,

$$\zeta 22 = 3B \left(C_1 \left(Bt^\beta \right)^{\frac{1}{\beta}} \beta + t \Gamma\left[\frac{1}{\beta}, Bt^\beta\right] \right)$$
$$\times \left({}^{gg} C_1^2 \rho_{m_0} \left(Bt^\beta \right)^{2/\beta} \beta^2 \right.$$
$$\left. + 2C_1 \rho_{m_0} t \left(Bt^\beta \right)^{\frac{1}{\beta}} \beta \Gamma\left[\frac{1}{\beta}, Bt^\beta\right] + \rho_{m_0} t^2 \Gamma\left[\frac{1}{\beta}, Bt^\beta\right]^2 \right.$$

Fig. 7 Evolution of reconstructed effective EoS parameter of viscous BHDE in non-interacting intermediate scenario

$$+ c e^{Bt^\beta} \left(Bt^\beta \right)^{2/\beta} \beta^2$$
$$\times \left(e^{Bt^\beta} \left(C_1 + \frac{t \left(Bt^\beta \right)^{-1/\beta} \Gamma\left[\frac{1}{\beta}, Bt^\beta\right]}{\beta} \right) \right)^\Delta \right)$$

Here, we have plotted effective EoS parameter($w_{eff} = \frac{P+\Pi}{\rho_{Total}}$) in non-interacting intermediate scenario in Fig. 7. Figure 7 shows that phantom scenario of effective EoS parameter and this the reconstructed w_{eff} can not avoid the big-rip by exiting the phantom boundary. Now, from the definition of deceleration parameter ($q(t) = \frac{-\ddot{a}(t)}{aH^2}$) and square speed of sound against small perturbations ($c_s^2 = \frac{d(P_{effective})}{d(\rho_{Total})}$), we have examined our model's rate of expansion and stability in non-interacting intermediate scenario. In Fig. 8, accelerating expansion of the universe has been demonstrated and Fig. 9 shows that our model is stable for all values of Δ against small perturbations. Here, we have chosen β and B as positive parameters and $\beta \in (0, 1)$.
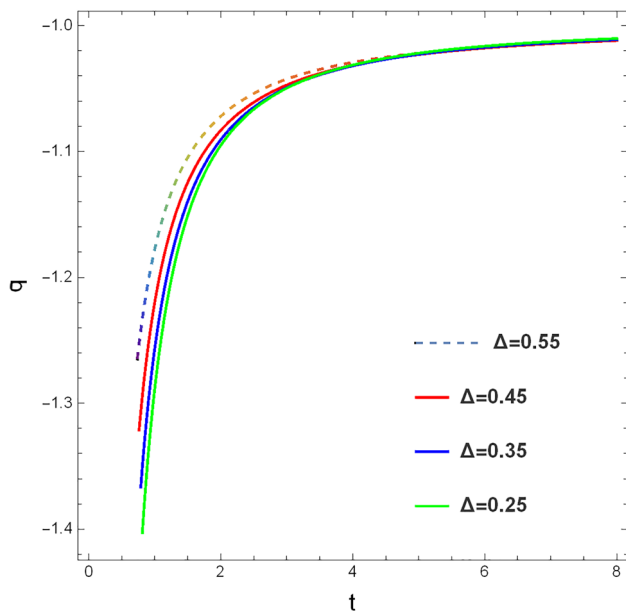
3.4.2 Intermediate BHDE universe: coupled fluid model

In this subsection, we have considered interacting scenario by taking interaction term $Q = 3Hb^2\rho_m$. Considering Eqs. (24), (25) and (28) we can get, ρ_m and EoS parameter in interacting scenario. Therefore,
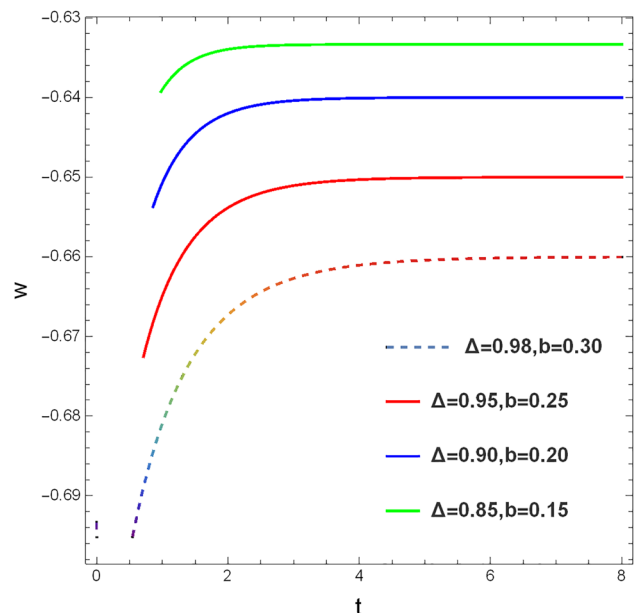
$$\rho_m = e^{3(-1+b^2)Bt^\beta} C_2,$$

(32)

Although,

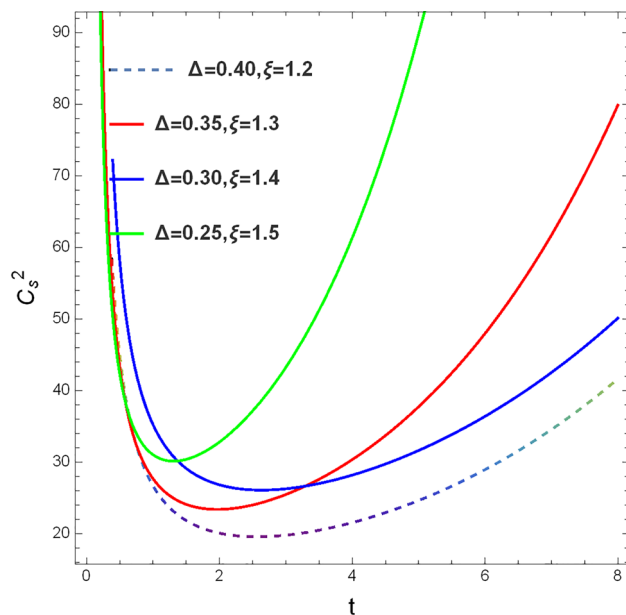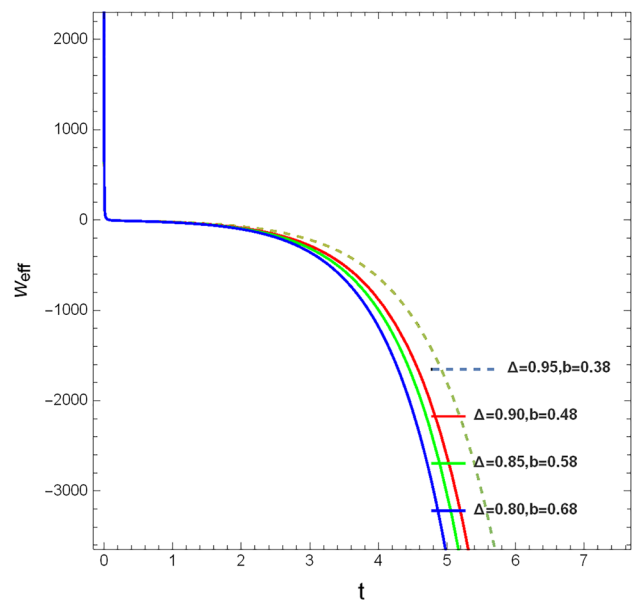$$\rho_{Total} = \rho_{BHDE} + \rho_m$$

(33)

Fig. 8 Evolution of deceleration parameter in non-interacting intermediate scenario

Fig. 10 Evolution of reconstructed viscous interacting EoS parameter for the range b lies in $(0, 1)$ in intermediate scenario

Fig. 9 Square speed of sound $c_s^2 \geq 0$ for viscous BHDE in non-interacting intermediate scenario

Fig. 11 Evolution of reconstructed viscous interacting effective EoS parameter for the range b lies in $(0, 1)$ in intermediate scenario

Hence, from Eqs. (7), (33) and $\Pi = -3\xi H^2$ we can get, thermodynamic pressure, EoS parameter and effective EoS parameter respectively. In Figs. 10 and 11 we have plotted viscous interacting EoS parameter and effective EoS parameter of reconstructed BHDE in intermediate scenario respectively. We can see quintessence behavior of EoS parameter in Fig. 10 and effective EoS parameter is firmly approaching the phantom border in Fig. 11. It is established that our model is stable against small perturbations with background

fluid as BHDE in interacting viscous intermediate scenario by square speed of sound test.

3.4.3 Bouncing cosmologies: general characteristics

In this case, the density of BHDE has been regarded as

$$\rho_{BHDE} = cR_E^{\Delta-2}$$

in which Δ is higher than 0 and c is the model's component, and in the case of a bouncing universe,

$$a(t) = a_0 e^{\mu t} + a_1 e^{-\gamma t}$$

where the positive real values μ, γ, a_0, and a_1 are listed. By the reference of $\dot{a}(t) = a_0 \mu e^{\mu t} - a_1 \gamma e^{-\gamma t}$ we can get, Hubble parameter as Eq. (14). Therefore, in this bouncing universe, using bouncing Hubble parameter (14) in $\dot{R}_E = H R_E - 1$, we can get,

$$R_E = \frac{e^{-tv}\left(a_1 + a_0 e^{t(\mu+v)}\right)\left(a_1 v C_1 - e^{tv}{}_2F_1\left[1, \frac{v}{\mu+v}, \frac{\mu+2v}{\mu+v}, -\frac{a_0 e^{t(\mu+v)}}{a_1}\right]\right)}{a_1 v} \tag{34}$$

Therefore, reconstructed energy density of BHDE in bouncing scenario be:

$$\rho_{BHDE} = c\left(\frac{e^{-tv}\left(a_1 + a_0 e^{t(\mu+v)}\right)\left(a_1 v C_1 - e^{tv}{}_2F_1\left[1, \frac{v}{\mu+v}, \frac{\mu+2v}{\mu+v}, -\frac{a_0 e^{t(\mu+v)}}{a_1}\right]\right)}{a_1 v}\right)^{-2+\Delta} \tag{35}$$

We already postulated the existence of both the perfect fluid of ordinary matter and the previously described viscous Barrow holographic dark energy in the universe as a whole.

3.4.4 Bounce BHDE universe: single fluid model

We have examined the bounce non-interacting case in this subsection. Consequently, we may obtain the density of pressure-less dark matter from Eq. (17).

$$\rho_m = \frac{\rho_{m_0}}{\left(a_0 e^{t\mu} + a_1 e^{-tv}\right)^3} \tag{36}$$

Thus, we can obtain the equation of ρ_{Total} from Eqs. (35) and (36).

$$\rho_{Total} = \frac{\rho_{m_0}}{\left(a_0 e^{t\mu} + a_1 e^{-tv}\right)^3} + c\left(\frac{e^{-tv}\left(a_1 + a_0 e^{t(\mu+v)}\right)\left(a_1 v C_1 - e^{tv}{}_2F_1\left[1, \frac{v}{\mu+v}, \frac{\mu+2v}{\mu+v}, -\frac{a_0 e^{t(\mu+v)}}{a_1}\right]\right)}{a_1 v}\right)^{-2+\Delta} \tag{37}$$

Therefore, from Eq. (7) and $\Pi = -3\xi H^2$, we can get the expression of thermodynamic pressure of BHDE and EoS parameter,

$$P = \frac{1}{3}\left(-\frac{\rho_{m_0}}{\left(a_0 e^{t\mu} + a_1 e^{-tv}\right)^3} - \frac{6\left(a_0 e^{t(\mu+v)}\mu^2 + a_1 v^2\right)}{a_1 + a_0 e^{t(\mu+v)}} + \frac{9\left(a_0 e^{t(\mu+v)}\mu - a_1 v\right)^2 \xi}{\left(a_1 + a_0 e^{t(\mu+v)}\right)^2} \right.$$

$$\left. -c\left(\frac{e^{-tv}\left(a_1 + a_0 e^{t(\mu+v)}\right)\left(a_1 v C_1 - e^{tv}{}_2F_1\left[1, \frac{v}{\mu+v}, \frac{\mu+2v}{\mu+v}, -\frac{a_0 e^{t(\mu+v)}}{a_1}\right]\right)}{a_1 v}\right)^{-2+q\Delta}\right) \tag{38}$$

$$w = \left(a_1^2 c e^{2t\nu} \nu^2 \left(\frac{e^{-t\nu}\left(a_1 + a_0 e^{t(\mu+\nu)}\right)\left(a_1 C_1 \nu - e^{t\nu}{}_2F_1\left[1, \frac{\nu}{\mu+\nu}, \frac{\mu+2\nu}{\mu+\nu}, -\frac{a_0 e^{t(\mu+\nu)}}{a_1}\right]\right)}{a_1 \nu} \right)^{\Delta} \right.$$

$$\times \left(a_1\nu\left(-e^{t\nu}(-2+\Delta) + a_0 C_1 e^{t(\mu+\nu)}(1+\Delta)\mu - a_1 C_1(1+\Delta)\nu\right) \right.$$

$$\left. -(1+\Delta)\left(a_0 e^{t(\mu+2\nu)}\mu - a_1 e^{t\nu}\nu\right){}_2F_1\left[1, \frac{\nu}{\mu+\nu}, \frac{\mu+2\nu}{\mu+\nu}, -\frac{a_0 e^{t(\mu+\nu)}}{a_1}\right]\right) \right) \Big/$$

$$\times \left(3\left(a_1 + a_0 e^{t(\mu+\nu)}\right)^2\left(a_0 e^{t(\mu+\nu)}\mu - a_1\nu\right)\left(-a_1 C_1 \nu + e^{t\nu}{}_2F_1\left[1, \frac{\nu}{\mu+\nu}, \frac{\mu+2\nu}{\mu+\nu}, -\frac{a_0 e^{t(\mu+\nu)}}{a_1}\right]\right)^3 \right.$$

$$\times \left.\left(\frac{\rho_{m_0}}{\left(a_0 e^{t\mu} + a_1 e^{-t\nu}\right)^3} + c\left(\frac{e^{-t\nu}\left(a_1 + a_0 e^{t(\mu+\nu)}\right)\left(a_1 C_1 \nu - e^{t\nu}{}_2F_1\left[1, \frac{\nu}{\mu+\nu}, \frac{\mu+2\nu}{\mu+\nu}, -\frac{a_0 e^{t(\mu+\nu)}}{a_1}\right]\right)}{a_1 \nu} \right)^{-2+\Delta} \right) \right) \tag{39}$$

and, we know that $w_{eff} = \frac{P+\Pi}{\rho_{Total}}$, therefore,

$$w_{eff} = -\frac{\zeta_{31}}{\zeta_{32}} \tag{40}$$

where,

the symmetry of the graphs surrounding the bouncing point. There is a continuous and stabilized background evolution of the energy density. At $t = 0$, the bounce is confirmed and is clearly visible. Figure 13 illustrates how the EoS parameter crosses the phantom border in both the cases pre and

$$\zeta_{31} = \frac{3\left(a_0 e^{t(\mu+\nu)}\mu - a_1\nu\right)^2 \xi}{\left(a_1 + a_0 e^{t(\mu+\nu)}\right)^2}$$

$$+\frac{1}{3}\left(\frac{\rho_{m_0}}{\left(a_0 e^{t\mu} + a_1 e^{-t\nu}\right)^3} + \frac{6\left(a_0 e^{t(\mu+\nu)}\mu^2 + a_1\nu^2\right)}{a_1 + a_0 e^{t(\mu+\nu)}} - \frac{9\left(a_0 e^{t(\mu+\nu)}\mu - a_1\nu\right)^2 \xi}{\left(a_1 + a_0 e^{t(\mu+\nu)}\right)^2} \right.$$

$$+\left. c\left(\frac{e^{-t\nu}\left(a_1 + a_0 e^{t(\mu+\nu)}\right)\left(a_1 \nu C_1 - e^{t\nu}{}_2F_1\left[1, \frac{\nu}{\mu+\nu}, \frac{\mu+2\nu}{\mu+\nu}, -\frac{a_0 e^{t(\mu+\nu)}}{a_1}\right]\right)}{a_1 \nu} \right)^{-2+\Delta} \right)$$

$$\zeta_{32} = \frac{\rho_{m_0}}{\left(a_0 e^{t\mu} + a_1 e^{-t\nu}\right)^3} + c\left(\frac{e^{-t\nu}\left(a_1 + a_0 e^{t(\mu+\nu)}\right)\left(a_1 \nu C_1 - e^{t\nu}{}_2F_1\left[1, \frac{\nu}{\mu+\nu}, \frac{\mu+2\nu}{\mu+\nu}, -\frac{a_0 e^{t(\mu+\nu)}}{a_1}\right]\right)}{a_1 \nu} \right)^{-2+\Delta}.$$

Additionally, we showed total energy density (ρ_{Total}), the EoS parameter, and effective EoS parameter in the non-interacting bouncing scenario in Figs. 12, 13, and 14 respectively. The universe's proper chronological growth is seen in Fig. 12. The BHDE energy density in Fig. 12 decreases due to contraction in the pre-bounce scenario, reaches its lowest value at $t = 0$ during the bounce, and rises due to expansion in the post-bounce scenario. According to the inflationary hypothesis of the universe, this illustration depicts a rapid increase in density brought on by bounce inflation, followed by stability of density across succeeding eras of the cosmos. The existence of t^2 in the associated formulas accounts for

post-bounce scenario. The reconstructed w_{eff}, effective EoS parameter is behaving quintessence in pre-bounce scenario and phantom in post bounce scenario as seen in Fig. 14, and the phantom scenario of the effective EoS parameter can escape the big-rip in post bounce scenario.

We have now investigated the rate of expansion and stability of our model in a non-interacting bouncing situation, starting from the specification of the deceleration parameter ($q(t) = \frac{-\ddot{a}(t)}{aH^2}$) and the square speed of sound against minor perturbations ($c_s^2 = \frac{d(P_{effective})}{d(\rho_{Total})}$). The universe's accelerating expansion is illustrated in Figs. 15, and 16 demonstrates that
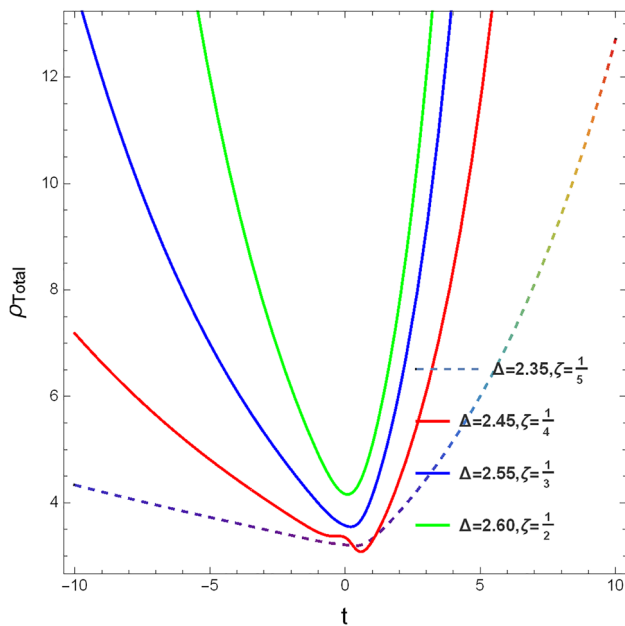
Fig. 12 Evolution of reconstructed viscous total BHDE density in the non-interacting bouncing scenario

Fig. 13 Evolution of reconstructed EoS parameter of viscous BHDE in non-interacting bouncing scenario

our model is stable against tiny perturbations for all values of Δ in pre and post-bounce scenario.
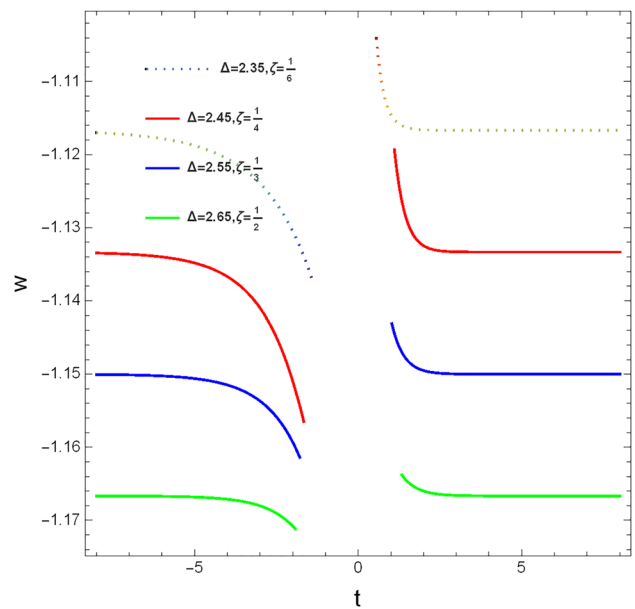
3.4.5 Bounce BHDE universe: coupled fluid model

In this part, we assume that the pressure-less DM and the dark fluids of the universe, BHDE and Q, exchange energy through an interaction term. We have taken the interaction term $Q = 3Hb^2\rho_m$ to explore an interacting scenario in the current section. Taking into account Eqs. (24), (25) and (35), we may obtain the ρ_m and EoS parameter in an interacting scenario.

$$\rho_m = e^{3(-1+b^2)(-tv+\log(a_1+a_0e^{t(\mu+v)}))}C_2 \qquad (41)$$

Again, we have taken, $\rho_{Total} = \rho_{DE} + \rho_m$ and therefore,

$$\rho_{Total} = C_2 e^{3(-1+b^2)(-tv+\log[a_1+a_0e^{t(\mu+v)}])}$$
$$+ c\left(\frac{e^{-tv}\left(a_1+a_0e^{t(\mu+v)}\right)\left(a_1C_1v - e^{tv}{}_2F_1\left[1, \frac{v}{\mu+v}, \frac{\mu+2v}{\mu+v}, -\frac{a_0e^{t(\mu+v)}}{a_1}\right]\right)}{a_1 v}\right)^{-2+\Delta} \qquad (42)$$

Therefore, from $\dot{\rho}_{DE} + 3H\rho_{DE}(1+w) + 3Hb^2\rho_m = 0$, we can get the expression of EoS parameter and effective EoS parameter in viscous, interacting, bouncing scenario. As a result, as shown in Fig. 17, the growth of the reconstructed EoS parameter (left panel) diverges as the denominator is zero at the bouncing point $t = 0$ in the equation of the EoS parameter. In the post-bounce instance, the EoS parameter crosses the phantom boundary at early stages, but later

it behaves like a quintessence scenario; in the pre-bounce case, it behaves like a quintessence scenario depending on the interaction coefficient. In the post-bounce scenario, the Big Rip singularity is avoided by the effective EoS parameter in Fig. 18 (right panel). It is evident that both EoS parameters are strictly moving to phantom when we increase the interaction coefficient b.

4 Barrow holographic dark fluid-driven inflation

One key challenge for inflation is the singularity problem before the onset of inflation itself. Therefore, the full history of the very early the universe cannot be obtained from the inflationary model. This singularity problem is automatically avoided in a bouncing cosmic scenario, but at the expense of requiring the introduction of new physics to achieve the bounce. Non-singular bouncing cosmologies are a contemporary alternative to the inflationary Big-Bang scenario. These cosmologies, in general, offer geodesic completeness and address certain issues that inflation was designed to resolve, such the horizon problem. Inspired by the studies [113–116,141,142], we are going to discuss a scenario where
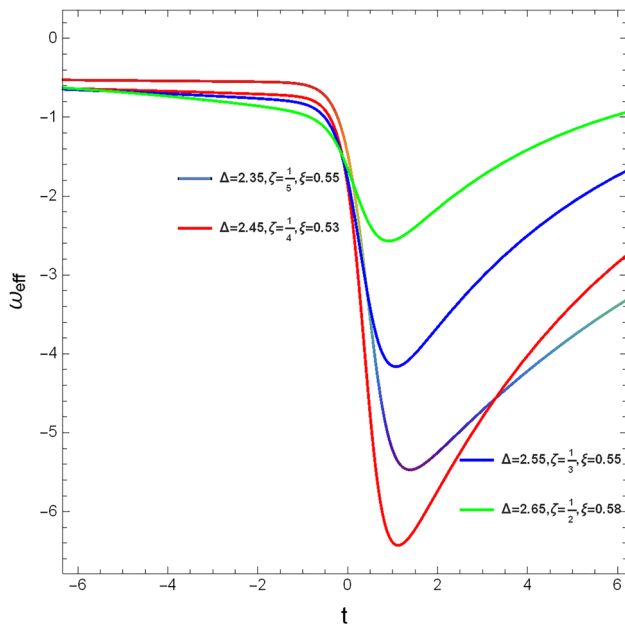
Fig. 14 Evolution of reconstructed effective EoS parameter of viscous BHDE in the non-interacting bouncing scenario

Fig. 15 Evolution of deceleration parameter in non-interacting bouncing scenario

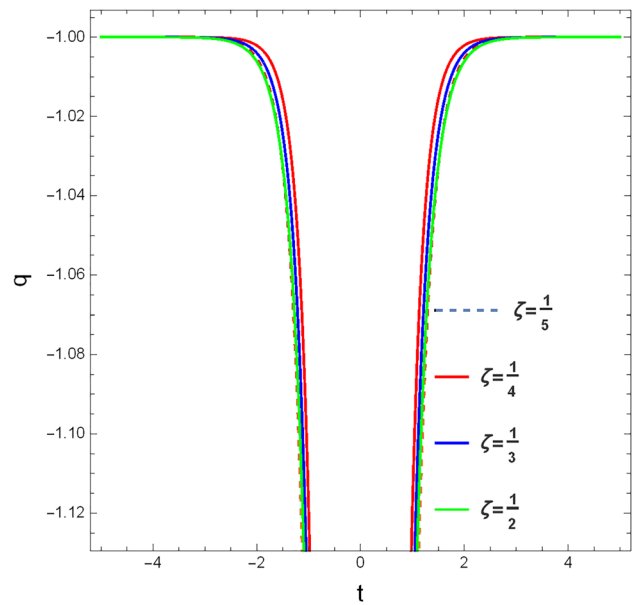**Fig. 16** Square speed of sound $c_s^2 \geq 0$ for viscous BHDE in non-interacting bouncing scenario

there is a transition to accelerated expansion at the end of a non-singular bounce. For a general inflation scenario, the initial Friedmann equation can be expressed as $H^2 = \frac{\rho_{inf}}{3}$, where, ρ_{inf} represents the density of energy of the (effective) fluid that drives inflation, which can come from numerous sources and mechanisms as well as a scalar field or modified gravity. Please take note that we have, as usual, overlooked the contributions made by the radiation components. In this study, we examine the possibility that inflation has a Barrow holographic origin, meaning that non-interacting pressure-less dark matter and the Barrow holographic energy density serve as its source. Because $\rho_{inf} = \rho_{Total}$, it follows that $\rho_{Total} = \rho_m + \rho_{BHDE}$.

4.1 Hubble slow-roll approximation

Here, the Hubble slow-roll parameters ϵ_n (with n being a positive integer) [143–146] can consequently be obtained as the evolution of $H(t)$ is known in emergent, intermediate situation. Therefore,

$$\epsilon_{n+1} = \frac{d \ln|\epsilon_n|}{dN} \tag{43}$$

along with $\epsilon_0 = \frac{H_{initial}}{H}$ and the e-folding number N is defined as, $N = \ln(\frac{a}{a_{initial}})$. Here, $a_{initial}$ be the scale factor at the beginning of inflation corresponding to Hubble parameter at that time be $H_{initial}$. Again, using k as the absolute value of the wave number k, we can compute the values of the inflationary observables, which are the tensor spectral index n_T, the tensor-to-scalar ratio r, and the scalar spectral
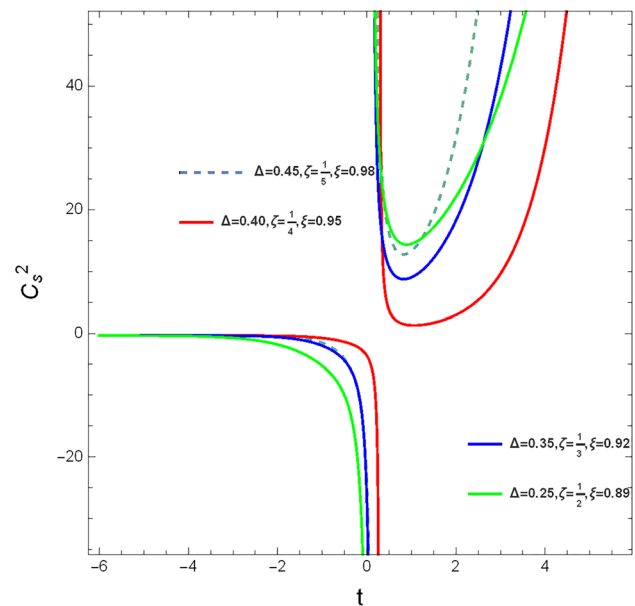
index of the curvature perturbations n_s, as reported in [145]. Therefore,
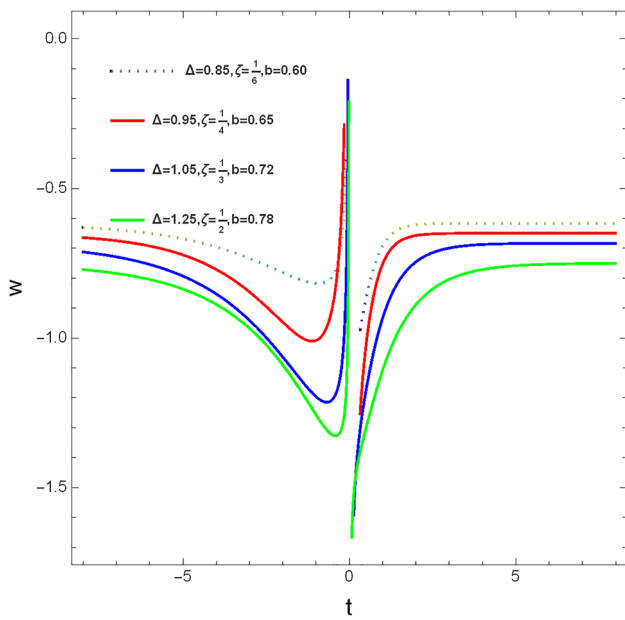
$$r \equiv 16\epsilon_1 \tag{44}$$

$$n_s \equiv 1 - 2\epsilon_1 - 2\epsilon_2 \tag{45}$$

$$\alpha_s \equiv -2\epsilon_1\epsilon_2 - \epsilon_2\epsilon_3 \tag{46}$$

$$n_T \equiv -2\epsilon_1 \tag{47}$$

where, the first three Hubble slow-roll parameters are-

Fig. 17 Evolution of reconstructed viscous interacting EoS parameter in bouncing scenario

$$\epsilon_1 = \frac{-\dot{H}}{H^2} \tag{48}$$

$$\epsilon_2 = \frac{\ddot{H}}{H\dot{H}} - \frac{2\dot{H}}{H^2} \tag{49}$$

should, in theory, perform a full perturbation analysis for this particular Barrow holographic model in order to extract the exact expressions for the inflationary observable. However, the approximate relations Eqs. (44-47), which hold for all scenarios provided $H(t)$ is known for emergent and intermediate scenario, are sufficient for the sake of the current study [145] to provide the estimated values for the inflationary observable. Relationships Eqs. (44-47) are highly helpful since they let one compare data and Barrow holographic inflation predictions.

4.1.1 Hubble slow-roll approximation in emergent universe

We now evaluate the slow-roll approximation's intrinsic structure. The basic principle of the horizon flow formalism is the inclusion of a set of flow parameters that describe the evolution of the Hubble scale. We know that,

$$\dot{H} = \frac{-1}{2}(\rho_{Total} + P + \Pi) \tag{51}$$

and,

$$H^2 = \frac{1}{3}(\rho_{Total}) \tag{52}$$

Therefore, by considering the emergent universe from Eq. (20), thermodynamic pressure and bulk-viscous pressure $\Pi = -3\xi H^2$, we can get the Hubble flow slow-roll parameters in the background of BHDE fluid.

$$
\epsilon_1 = -\frac{3}{c}\left(C_1 \left(\frac{e^{\frac{N}{n}}}{p}\right)^n + \frac{\left(1 + \frac{p\lambda}{e^{\frac{N}{n}} - p\lambda}\right)^n {}_2F_1\left[n,n,1+n,\frac{p\lambda}{-e^{\frac{N}{n}}+p\lambda}\right]}{n\mu} \right)^{2-\Delta}
$$
$$
\times \left(\frac{\left(\frac{e^{\frac{N}{n}}}{p}\right)^{-3n}\rho_{m_0}}{6a_0^3} + e^{-\frac{2N}{n}}np\lambda\left(e^{\frac{N}{n}} - p\lambda\right)\mu^2 + e^{-\frac{2N}{n}}n^2\left(e^{\frac{N}{n}} - p\lambda\right)^2\mu^2 \right.
$$
$$
\times \left. -\frac{1}{3}c\left(C_1 \left(\frac{e^{\frac{N}{n}}}{p}\right)^n + \frac{\left(1 + \frac{p\lambda}{e^{\frac{N}{n}} - p\lambda}\right)^n {}_2F_1\left[n,n,1+n,\frac{p\lambda}{-e^{\frac{N}{n}}+p\lambda}\right]}{n\mu} \right)^{-2+\Delta} \right) \tag{53}
$$

$$\epsilon_3 = (\ddot{H}H - 2\dot{H}^2)^{-1} * \left[\frac{H\dot{H}\dddot{H} - \ddot{H}(\dot{H}^2 + H\ddot{H})}{H\dot{H}} \right.$$
$$\left. -\frac{2\dot{H}}{H^2}(H\ddot{H} - 2\dot{H}^2) \right] \tag{50}$$

We note here that, based on the thorough perturbation analysis of holographic dark energy carried out in [147], we

Rather than addressing the perturbation analysis of BHDE, the standard perturbation strategy for obtaining the scalar spectral index, n_s, and tensor-to-scalar ratio, r, is used as the approximation methodology by considering Eqs. (20, 44, 45, 46, 47). Here, the standard perturbation technique serves as a useful approximation. The process outlined above is used to determine the n_s and r at the horizon crossing, demonstrating their dependence on the model's free constants.

The evolution of ϵ_1 with respect to e-folding number(N) and tensor to scalar ratio r against spectral index n_s in viscous emergent scenario is plotted in Figs. 19 and 20 respectively. We can see, the inflationary scenario and nice exit from inflation ($\epsilon_1 = 1$) in Fig. 19. During the inflationary era, ($\epsilon_1 = 1$) has the largest value. After leaving the inflationary phase, it exhibits negative behaviour. It is observed that the trajectories in (n_s, r) plane exhibit a decreasing behaviour, which is consistent Planck2018 data set. Hence, our calculated tensor to scalar ratio for this model is consistent with the observational bound of Planck. Hence, it can explain the primordial fluctuation in the early universe.

4.1.2 Hubble slow-roll approximation in intermediate universe

In this subsection, we have considered an intermediate scale factor to incorporate Hubble flow dynamics in the background of the BHDE universe. Here, we have taken matter density with Barrow holographic dark energy density for the evolution of the Hubble parameter. We substitute ρ and P in Eq. (51) for finding $\dot{H}$ by ρ_{Total} of non-interacting viscous total energy density and $P + \Pi$ effective pressure respectively in the intermediate universe. Therefore,

Therefore, from $\epsilon_2 = \frac{\dot{\epsilon}}{H\epsilon_1}$ and Eq. (54), we can calculate, tensor to scalar ratio and spectral index in this intermediate scenario. Here, we define all the slow-roll parameters in terms of H, which is a function of the number of e-folds N during inflation and may be written as $H = H(N)$. The scalar spectral index, often represented as (n_s), explains the scale dependence of density variations. When there is an index of unity, all scales have the same variances. The distinctive size scales of structure creation are influenced by the input parameter (n_s) of Λ_{CDM}, where a modest modification has minimal impact. Certain numbers (often ranges) of (n_s) are often suggested by inflationary models, and $n_s = 0.96$ is still very consistent with inflation models where it exists today. In this study, we give an exact constraint on fundamental gravitational waves, which is, tensor-to-scalar ratio (r), for a broad category of single-field inflation models in which, in the BHDE scenario, inflation always takes place below the Planck scale.

In this Fig. 21, we can define a successful inflationary phase (as $\epsilon_1 < 1$) in the viscous non-interacting intermediate universe with BHDE background fluid. There is a nice exit of the inflationary phase in this case. However, we have shown that the original model of inflation using viscous intermediate scale factor with BHDE background fluid is inconsistent with constraints on r and n_s at greater than 95% confidence

$$
\epsilon_1 = -\frac{1}{2c} \left(\left(e^{B\left(\left(\frac{-C_3+N}{B}\right)^{\frac{1}{\beta}}\right)^{\beta}} \left(C_1 + \frac{\left(\frac{-C_3+N}{B}\right)^{\frac{1}{\beta}} \left(B\left(\left(\frac{-C_3+N}{B}\right)^{\frac{1}{\beta}}\right)^{\beta}\right)^{-1/\beta} \Gamma\left[\frac{1}{\beta}, B\left(\left(\frac{-C_3+N}{B}\right)^{\frac{1}{\beta}}\right)^{\beta}\right]}{\beta} \right) \right)^{2-\Delta} \right.
$$

$$
\times \left(6B\left(\frac{-C_3+N}{B}\right)^{-2/\beta} \left(\left(\frac{-C_3+N}{B}\right)^{\frac{1}{\beta}}\right)^{\beta} \beta \left(-1 + \beta + B\left(\left(\frac{-C_3+N}{B}\right)^{\frac{1}{\beta}}\right)^{\beta} \beta \right) \right)
$$

$$
\times \left. -\frac{2ce^{-2B\left(\left(\frac{-C_3+N}{B}\right)^{\frac{1}{\beta}}\right)^{\beta}} \left(e^{B\left(\left(\frac{-C_3+N}{B}\right)^{\frac{1}{\beta}}\right)^{\beta}} \left(C_1 + \frac{\left(\frac{-C_3+N}{B}\right)^{\frac{1}{\beta}} \left(B\left(\left(\frac{-C_3+N}{B}\right)^{\frac{1}{\beta}}\right)^{\beta}\right)^{-1/\beta} \Gamma\left[\frac{1}{\beta}, B\left(\left(\frac{-C_3+N}{B}\right)^{\frac{1}{\beta}}\right)^{\beta}\right]}{\beta} \right) \right)^{\Delta}}{\left(C_1 + \frac{\left(\frac{-C_3+N}{B}\right)^{\frac{1}{\beta}} \left(B\left(\left(\frac{-C_3+N}{B}\right)^{\frac{1}{\beta}}\right)^{\beta}\right)^{-1/\beta} \Gamma\left[\frac{1}{\beta}, B\left(\left(\frac{-C_3+N}{B}\right)^{\frac{1}{\beta}}\right)^{\beta}\right]}{\beta} \right)^2} \right)
$$

(54)

interval. Slightly far from $n_s = 0.965$ and $r = 0.15$, the slow-roll formulas are not valid with respect to Planck2018 dataset and we display it in Fig. 22 for indicative purposes only.

4.2 Correspondence between BHDE and scalar field

In the next section, we demonstrate how the BHDE approach can be used to characterize inflationary behaviour in terms of two distinct scalar field dynamics. Bamba et al. [148] demonstrate a work which corresponds between DE and scalar field. Beginning with inflation, scalar field dynamics has been essential for modern cosmology, producing a paradigm shift that has integrated cosmology and high-energy physics. The scalar field dynamics with BHDE background fluid in the absence of background dark matter are introduced in the following.

4.2.1 Canonical scalar field

First, the relationship between the canonical scalar field and BHDE is examined. Mohammadi et al. [149] states that the canonical scalar field's pressure and energy density are as follows:

$$\rho_{\phi_{\tilde{c}}} = \frac{1}{2}\dot{\phi}_{\tilde{c}}^2 + V(\phi_{\tilde{c}}) \tag{55}$$

$$P_{\phi_{\tilde{c}}} = \frac{1}{2}\dot{\phi}_{\tilde{c}}^2 - V(\phi_{\tilde{c}}) \tag{56}$$

where, canonical scalar field is represented by $\phi_{\tilde{c}}$. Therefore, we can write,

$$V(\phi_{\tilde{c}}) = \frac{1}{2}\rho_{BHDE}(1 - w_{BHDE}) \tag{57}$$

and,

$$\dot{\phi}_{\tilde{c}}^2 = \rho_{BHDE}(1 + w_{BHDE}) \tag{58}$$

(a) Cosmological dynamics of canonical scalar field in emergent universe

Substituting ρ_{BHDE} and w_{BHDE} in Eq. (57) by ρ_{Total} and w_{eff} of emergent viscous non-interacting scenario from Eqs. (20) and (21), we get the potential $V(\phi_{\tilde{c}})$ and we have plotted $V(\phi_{\tilde{c}})$ and $2V - \dot{\phi}_{\tilde{c}}^2$ in Figs. 23 and 24 respectively. In Fig. 23, the generated potential function from the canonical scalar field is presented against the e-folding number N. Various trajectories are produced for different Δ values in order to comprehend how the potential varies with the parameter. It is clear from the figure that the potential increases as the Hubble function increases. This result is consistent with the observations. As we study $2V - \dot{\phi}_{\tilde{c}}^2$, we observe that it is positive (see Fig. 24) with respect to N. However, in the vicinity of the increase of e-folding number, $2V - \dot{\phi}_{\tilde{c}}^2$ is nearly flat, although it starts increasing sharply; hence, we may consider it to be consistent with the inflationary expansion.
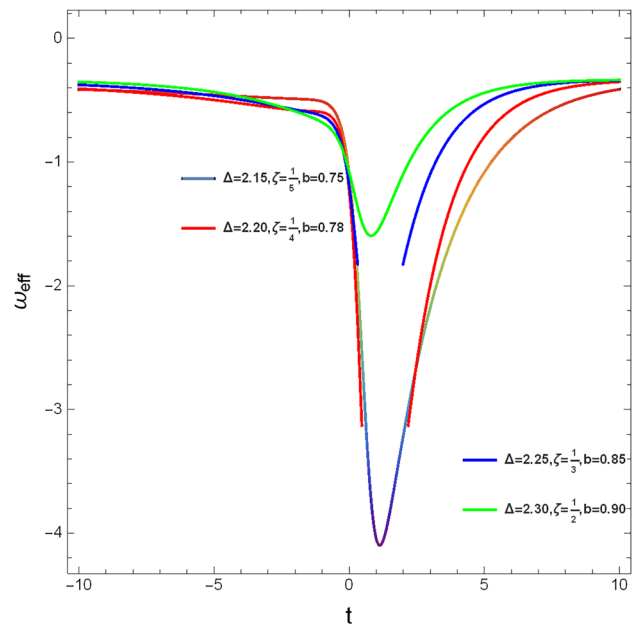
Fig. 18 Evolution of reconstructed viscous interacting effective EoS parameter in bouncing scenario
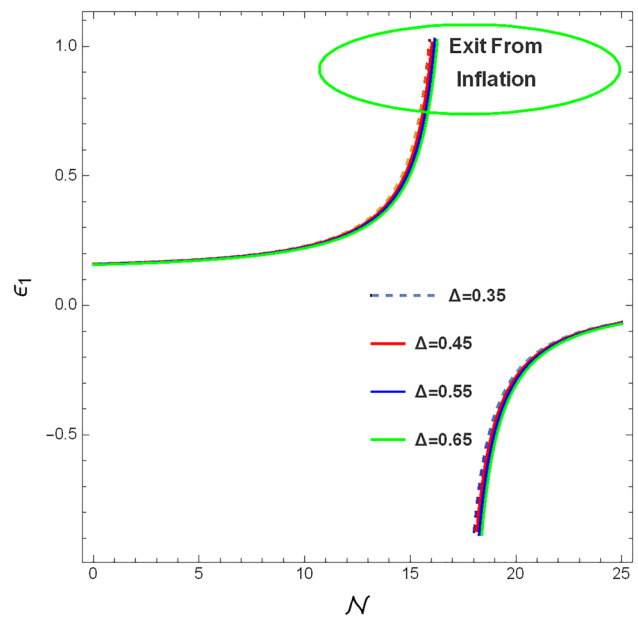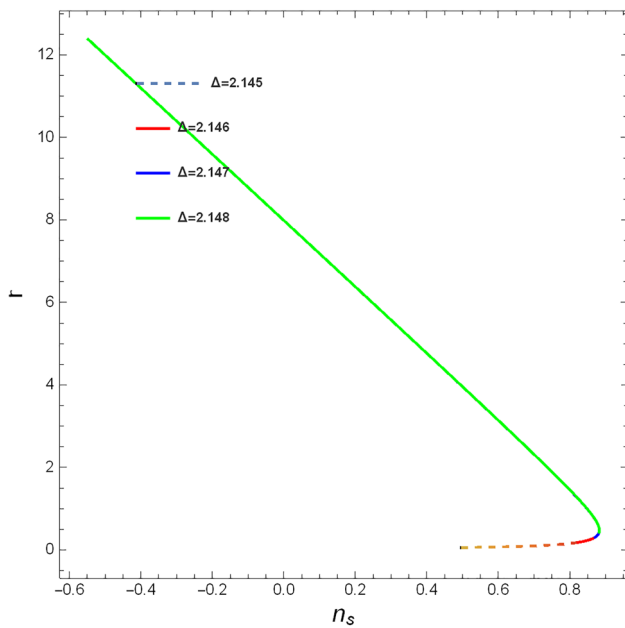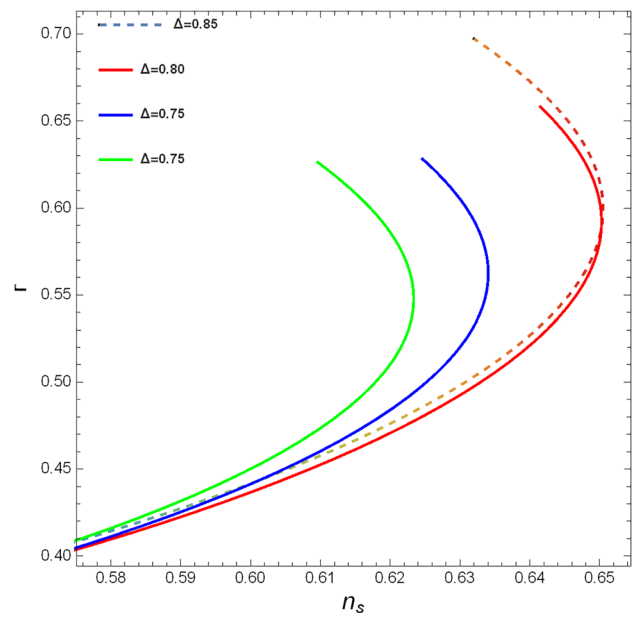

Fig. 19 Evolution of reconstructed Hubble flow parameter ϵ_1 with respect to e-folding number in viscous non-interacting emergent scenario

(b) Cosmological dynamics of canonical scalar field in intermediate universe

Inflationary scenarios refer to scenarios in which late-time acceleration and inflation are described by a single scalar field. A single scalar field is required for the consistent unification of inflation and late time acceleration with Big Bang singularity. This requires a potential that is initially followed by steep behaviour thereafter and shallow again around the

Fig. 20 Evolution of reconstructed tensor to scalar ratio r against spectral index n_s in viscous non-interacting emergent scenario for $\Delta \in (0, \infty)$

Fig. 22 Evolution of reconstructed tensor to scalar ratio r against spectral index n_s in viscous non-interacting intermediate scenario
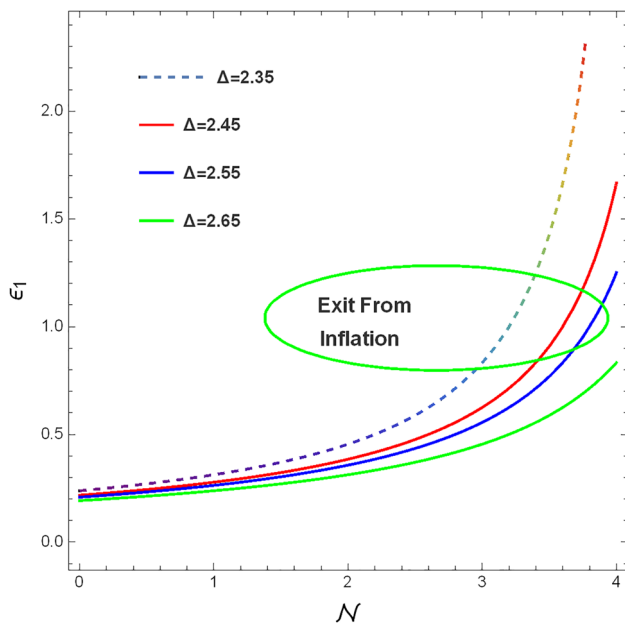
Fig. 21 Evolution of reconstructed Hubble flow parameter ϵ_1 with respect to e-folding number in viscous non-interacting intermediate scenario
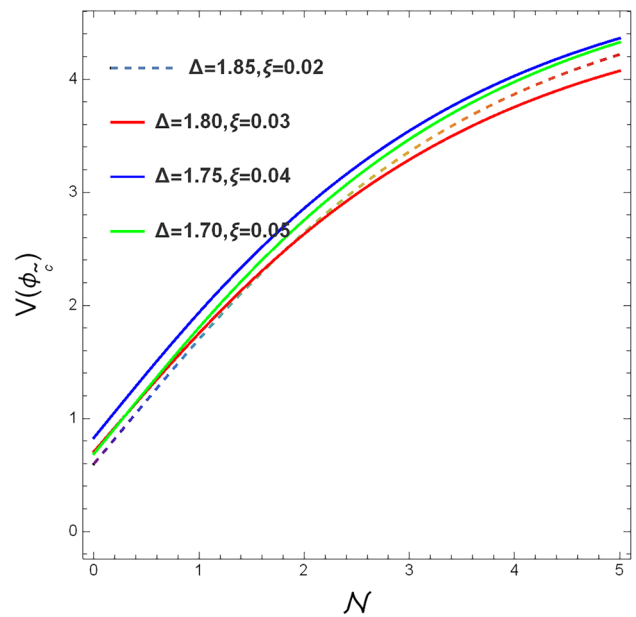
Fig. 23 Evolution of reconstructed canonical potential $V(\phi_{\tilde{c}})$ in viscous non-interacting emergent scenario

present epoch. When we replace ρ_{BHDE} and w_{BHDE} in Eq. (57) with ρ_{Total} and w_{eff} of the intermediate viscous non-interacting scenario, we obtain the $V(\phi_{\tilde{c}})$ like the previous case in Figs. 25 and 26, respectively, we have plotted $V(\phi_{\tilde{c}})$ and $2V - \dot{\phi}_{\tilde{c}}^2$.

The produced potential function from the canonical scalar field is shown against the e-folding number N in Fig. 25. To

understand how the potential fluctuates with the parameter, several trajectories are generated for various Δ values. With respect to N, $2V - \dot{\phi}_{\tilde{c}}^2$ is positive, as can be seen in Fig. 26. However, $2V - \dot{\phi}_{\tilde{c}}^2$ is almost flat near the e-folding number increase, as a result, we can see it as appropriate with the inflationary expansion.
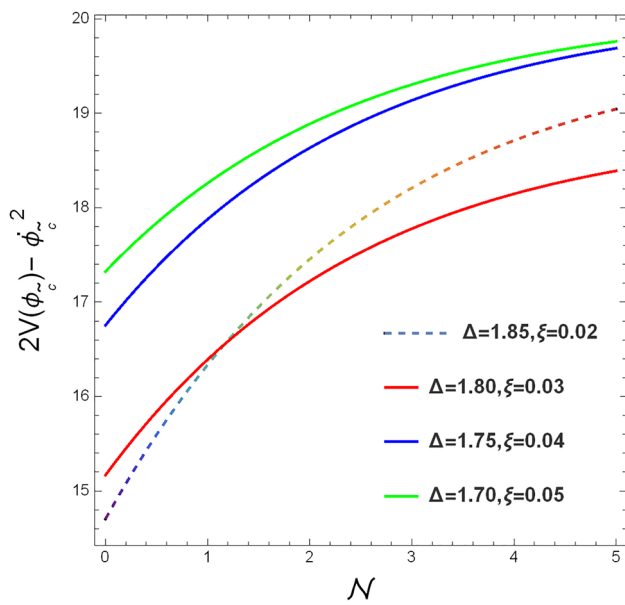
Fig. 24 Evolution of reconstructed $2V - \dot{\phi}_{\tilde{c}}^2$ in viscous non-interacting emergent canonical scalar field scenario
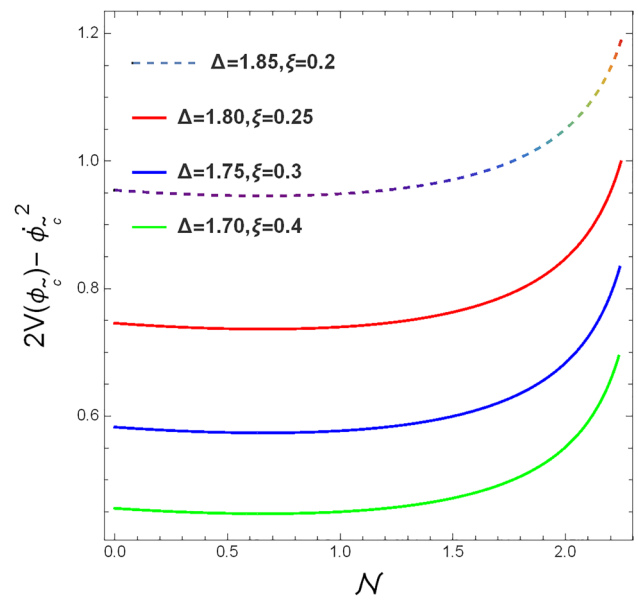
Fig. 26 Evolution of reconstructed $2V - \dot{\phi}_{\tilde{c}}^2$ in viscous non-interacting intermediate canonical scalar field scenario
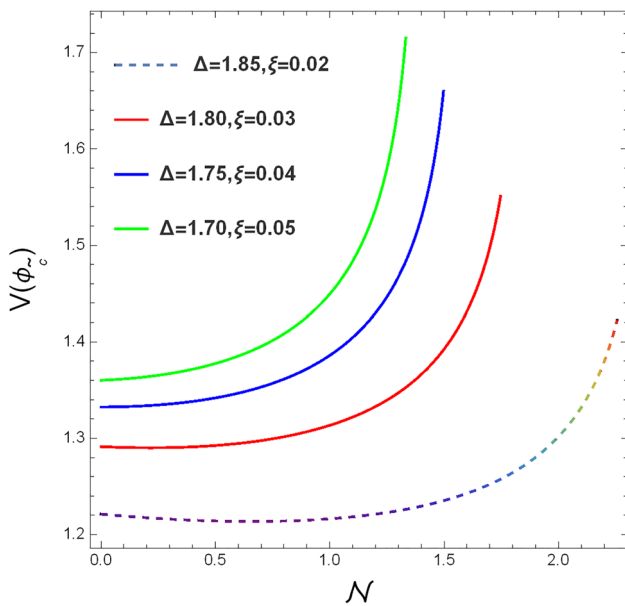
Fig. 25 Evolution of reconstructed canonical potential $V(\phi_{\tilde{c}})$ in viscous non-interacting intermediate scenario

4.2.2 Tachyonic field

In addition, tachyon fields [150] have been suggested as possible candidates for dark energy. Since tachyons are imaginary mass scalar fields, it is possible that they are never at rest and that their speed is always greater than that of light. In spite of this seemingly contradictory feature, models of tachyonic dark energy have been place up in which accelerated expansion is driven by the tachyon field. To make sure that these models are consistent with observational data and theoret-

ical constraints, they must be carefully examined because they involve complex dynamics. The purpose of this section is to look at the circumstances under which BHDE acts as a tachyonic field. For our investigation, an integrated approach seeks to identify common features, underlying principles, and potential connections between canonical and tachyonic scalar field models for our study. By creating such a framework, it may be possible to gain a better understanding of the nature of BHDE fluid and it provides a more comprehensive understanding of its role in the accelerated expansion of the universe with Big bang singularity as origin of the universe in this case. The tachyon field's pressure and energy density are determined by:

$$\rho_{\phi_{\tilde{T}}} = \frac{V(\phi_{\tilde{T}})}{\sqrt{1 - \dot{\phi}_{\tilde{T}}^2}} \tag{59}$$

$$P_{\phi_{\tilde{T}}} = -V(\phi_{\tilde{T}})\sqrt{1 - \dot{\phi}_{\tilde{T}}^2} \tag{60}$$

where, tachyonic scalar field is represented by $\phi_{\tilde{T}}$. In order to ascertain a suitable potential for the tachyonic field that exhibits BHDE behaviour, we evaluate the pressure and energy densities of these two dark energy models. The outcome is
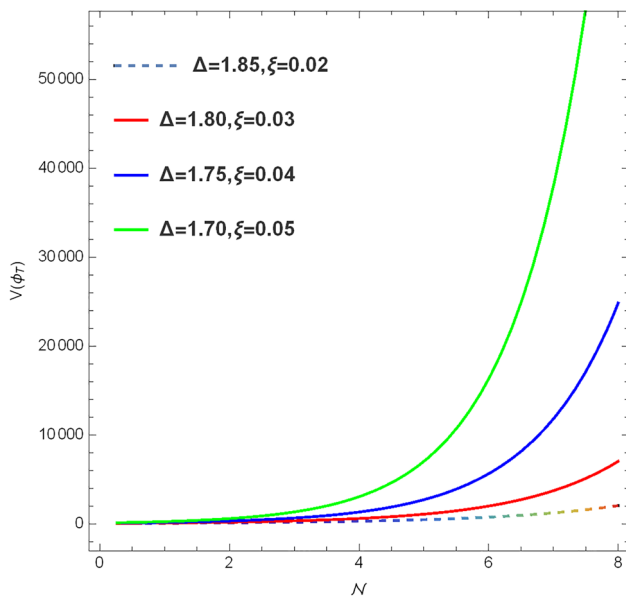
$$V(\phi_{\tilde{T}}) = \rho_{BHDE}\sqrt{1 - \dot{\phi}_{\tilde{T}}^2} \tag{61}$$

where,

$$\dot{\phi}_{\tilde{T}}^2 = 1 + w_{BHDE} \tag{62}$$

*(c) Cosmological dynamics of tachyonic scalar field in emergent universe*

Fig. 27 Evolution of reconstructed tachyon potential $V(\phi_{\tilde{T}})$ in viscous non-interacting emergent scenario

Fig. 28 Evolution of reconstructed $2V - \dot{\phi}_{\tilde{T}}^2$ in viscous non-interacting emergent tachyon scalar field scenario

Using ρ_{BHDE} and w_{BHDE} in Eqs. (61 and 62) by ρ_{Total} and w_{eff} respectively of emergent viscous non-interacting scenario from Eqs. (20) and (21), we get $V(\phi_{\tilde{T}})$ in terms of e-folding number N. Consequently, we can calculate $2V - \dot{\phi}_{\tilde{T}}^2$ in this tachyonic emergent scenario. We have plotted $V(\phi_{\tilde{T}})$ and $2V - \dot{\phi}_{\tilde{T}}^2$ in Figs. 27 and 28 respectively with respect to e-folding number N. Plotting the constructed potential function from the tachyonic scalar field against the e-folding number N is shown in Fig. 27. In this instance, distinct trajectories are produced for varying Δ values in order to comprehend how the potential depends on the parameter. This figure makes it clear that as the e-folding number increases, so does the potential. The observations are compatible with this outcome. In Fig. 28, we can see, $2V - \dot{\phi}_{\tilde{T}}^2$ is plotted with respect to e-folding number which is also consistent with the observational data as $2V >> \dot{\phi}_{\tilde{T}}^2$.

(d) Cosmological dynamics of tachyonic scalar field in intermediate universe

The motivations for using various scalar field dynamics in this study are rooted in their relevance to theoretical physics, cosmology. The tachyonic scalar field is frequently associated with scenarios involving dark energy or late-time accelerated expansion of the universe. Its exponential dependence on potential causes negative pressure and accelerates the universe's expansion in the late stages. The tachyonic scalar field is of particular interest for understanding the cosmic acceleration with intermediate scale factor, observed through supernovae and BHDE background fluid. Using ρ_{BHDE} and w_{BHDE} in Eqs. (61) and (62)) by ρ_{Total} and w_{eff} of intermediate viscous non-interacting scenario from Eq. (30) and effective EoS parameter, we obtain $V(\phi_{\tilde{T}})$
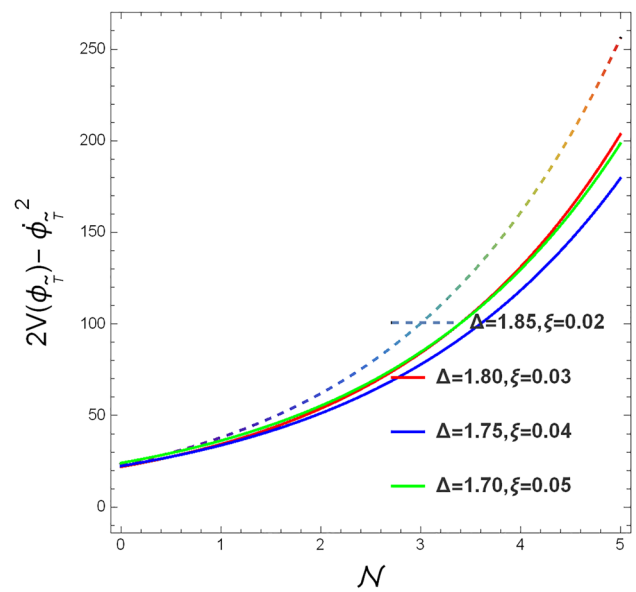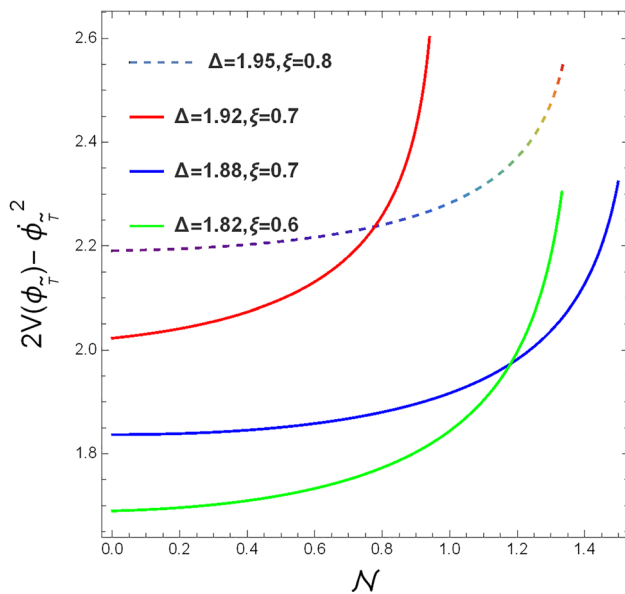
and hence $2V - \dot{\phi}_{\tilde{T}}^2$ in relation to e-folding number N. We plot $V(\phi_{\tilde{T}})$ and $2V - \dot{\phi}_{\tilde{T}}^2$ in Figs. 29 and 30, respectively. Figure 29 plots the constructed potential function from the tachyonic scalar field against the e-folding number N under the viscous BHDE as background fluid. Here, different trajectories are generated for different Δ and ξ values to understand the dependence of the potential on the parameter. This figure shows that the potential increases with the values of e-foldings. This conclusion is consistent with the observations. Plotting $2V - \dot{\phi}_{\tilde{T}}^2$ against e-folding number is shown in Fig. 30, and this is in compatible with the observational data, which shows that $2V >> \dot{\phi}_{\tilde{T}}^2$.

4.3 Inflation from bouncing scenario aspect

In contemporary theoretical cosmology, one of the most fundamental questions is whether the universe was singular or non-singular at its beginning. This inquiry is analogous to determining whether the Big Bang or Big Bounce theories adequately account for the universe's evolution. Our main objective for this study is to find a correlation between inflationary scenario following the Big Bang and rapid increase in volume after the Big Bounce, in the context of Einstein's gravity. This subsection is devoted on the study of bounce inflationary dynamics in various theoretical contexts. Traditionally, inflation was firstly studied in the context of scalar-tensor theory in its simplest form and we provide detailed calculations for the slow-roll indices, after getting the constraint range of bouncing parameters of this model for inflation in post bounce scenario. Then, we have found the correspondence between scalar fields and viscous non-interacting
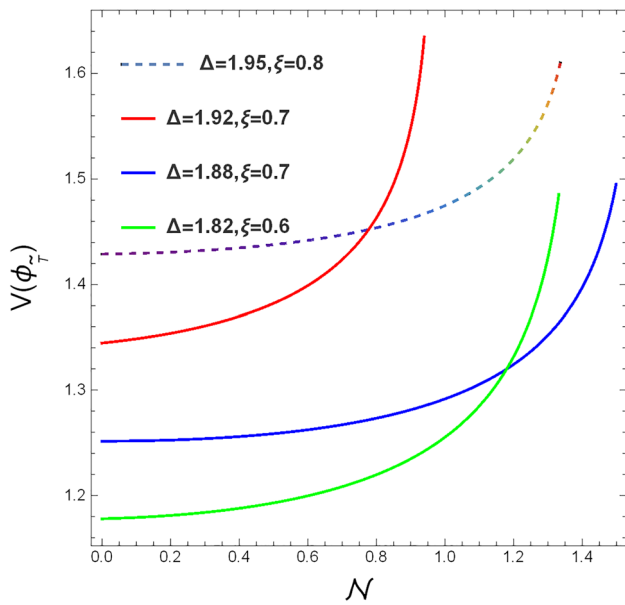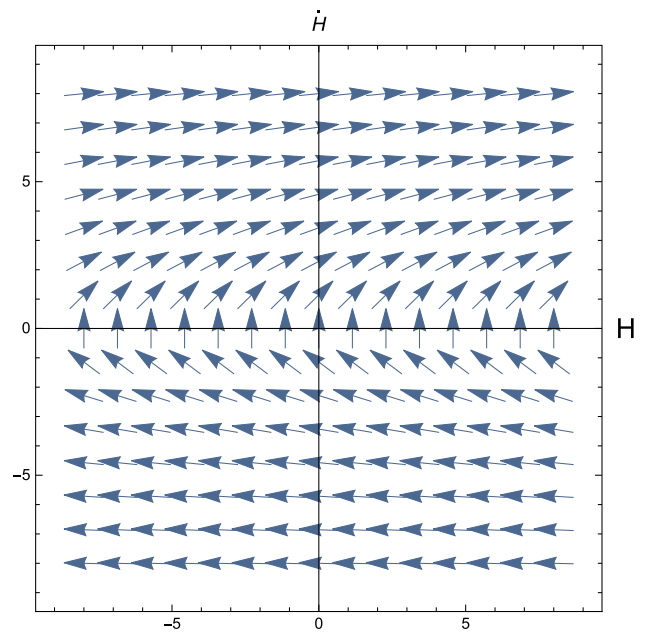
Fig. 29 Evolution of reconstructed tachyon potential $V(\phi_{\tilde{T}})$ in viscous non-interacting intermediate scenario
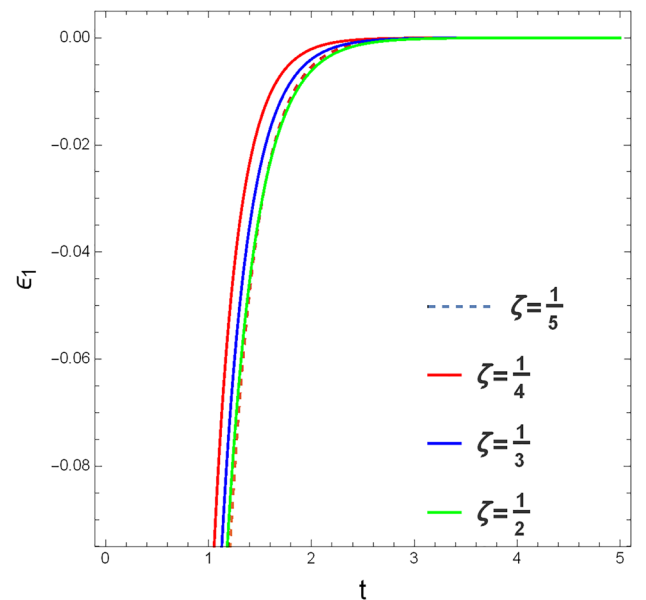

Fig. 31 $(\dot{H} - H)$ phase space diagram corresponds to Eq. (12): In the $\dot{H} > 0$, the bounce is at $H = 0$, where the transition from $H < 0$ to $H > 0$ is at $\dot{H} > 0$

Fig. 30 Evolution of reconstructed $2V - \dot{\phi}_{\tilde{c}}^2$ in viscous non-interacting intermediate tachyon scalar field scenario

Fig. 32 Evolution of reconstructed ϵ_1 in viscous non-interacting post bounce scenario

BHDE scenario, namely canonical scalar field and tachyonic scalar field. For completeness of bounce inflationary scenario, we first study the spectral index of primordial curvature perturbations and also the scalar-to-tensor ratio and then the canonical scalar field inflationary paradigm. In this same subsection, we study the tachyonic non-canonical scalar field case also.

4.3.1 Realisation of inflation in post-bounce scenario

To extract transparent and easily understandable information about the model at hand, we first construct the $(\dot{H} - H)$ phase space that corresponds to the bouncing scale factor Eq. (12) in viscous non-interacting BHDE scenario. In Fig. 31, we draw the phase space diagram $(\dot{H} - H)$ corresponding to Eq. (12), where the bounce point is evidently indicated at the

point ($H_B = 0$, $\dot{H} > 0$). Before this point, the contraction phase can be shown as $H < 0$ and $\dot{H} > 0$, while after this point the expansion phase is determined as $H > 0$ and $\dot{H} > 0$. Again, the effective EoS parameter can be re-written as $w_{eff} = \frac{-2\dot{H}}{3H^2} - 1$ from Eqs. (6, 7). Therefore, from Eqs. (12, 14), we can get,

$$w_{eff} = -1$$
$$- \frac{2a_0 e^{t(\mu+\nu)}(\mu+\nu)^3 \left(a_0 e^{t(\mu+\nu)}(-1+\mu) - a_1(1+\nu)\right)}{3(1+\nu)^2 \left(a_0 e^{t(\mu+\nu)}\mu - a_1\nu\right)^2}$$

(63)

Therefore, in the post-bouncing scenario, for an accelerating possible inflationary universe, the effective EoS parameter has to lie in the range of $(-1, \frac{-1}{3})$, which is the quintessence scenario. Therefore, in Eq. (63), $a_1(1+\nu) > a_0(-1+\mu)$ as the exponential function $e^{t(\mu+\nu)}$ always behaves positive for positive range of μ and ν. Therefore, to get $a_1(1+\nu) - a_0(-1+\mu) > 0$, μ has to lie $\mu \in (0, 1)$. In this case, we are taking a non-singular bounce with a bouncing point at $t = 0$ with the constraint $\frac{a_0}{a_1} = \frac{\gamma}{\mu} = \zeta$, in which ζ lies between $(0, 1)$. If μ is a proper fraction, then other parameters of Eq. (12), a_0, a_1, and ν have to be positive proper fractions for getting a post-bounce inflationary scenario. Again, we know that, the deceleration parameter $q = -1 - \frac{\dot{H}}{H^2}$, and first slow-roll parameter $\epsilon_1 = \frac{-\dot{H}}{H^2}$. For accelerating expansion of universe $q < -1$ and inflationary scenario $\epsilon_1 < 1$. Consequently, the accepting common region is $\frac{\dot{H}}{H^2} > 0$ for an accelerating inflationary scenario in the viscous non-interacting BHDE universe's post-bounce case. Furthermore, if all of the parameters of this double exponential bouncing model, a_0, a_1, μ and ν, belong to $(0, 1)$, the model can feel the inflationary phase gracefully in the quintessence period. Now, we have calculated Hubble flow parameters in the context of post-bounce viscous interacting scenario and illustrated the methods of spectral index of primordial curvature perturbations and also the scalar-to-tensor ratio. Therefore,

In Fig. 31 we have plotted phase space diagram of $\dot{H} - H$ and in Fig. 32 we have plotted the evolution of reconstructed ϵ_1 in post-bounce viscous interacting scenario. Figure 32 shows $\epsilon_1 \ll 1$ although we are unable to show the nice exit from bounce inflation.

4.3.2 Correspondence to the scalar field in bouncing scenario

Belinsky–Khalatnikov–Lifshitz (BKL) anisotropic instability is a well-known conceptual problem for bouncing cosmologies [151]. When the effective energy density caused by the back-reaction of anisotropies rises more quickly than the energy densities of the dust and radiation matter fields, the BKL instability manifests in contracting cosmologies. Therefore, to guarantee that anisotropies never dominate and to have a bounce that is approximately isotropic, the initial conditions must be fine-tuned to be almost perfectly isotropic. Anisotropies are justified to be ignored in the presence of an ekpyrotic scalar field because this problem is avoided in the ekpyrotic scenario, where a scalar field with a steep and negative-valued potential always dominates over anisotropies in a contracting universe [152]. A scalar field with a Horndeski-type non-standard kinetic term and a negative exponential potential has been shown to be able to combine an era of ekpyrotic contraction with a non-singular bounce [153]. Moreover, the matter bounce and the ekpyrotic scenario can be combined by assuming the universe started in a state of matter-dominated contraction and including a regular dust field. Within the framework of canonical and non-canonical tachyonic scalar fields with the viscous non-interacting BHDE scenario, we will examine the matter-ekpyrotic bounce in this paper. We will also compare its dynamics to those found in the effective field approach developed in [153]. In order to prevent the BKL instability and dilute anisotropy, it is imperative that a phase of Ekpyrotic contraction precedes the bounce, and this is achieved by

$$\epsilon_1 = \frac{3\frac{\rho_{m0}}{3(a_0 e^{t\mu} + a_1 e^{-t\nu})^3} - \frac{3a_0 e^{t(\mu+\nu)}\mu^2}{a_1 + a_0 e^{t(\mu+\nu)}} - \frac{3a_1\nu^2}{a_1 + a_0 e^{t(\mu+\nu)}} + c\left(\frac{e^{-t\nu}\left(a_1 + a_0 e^{t(\mu+\nu)}\right)\left(a_1 C_1 \nu - e^{t\nu} {}_2F_1\left[1, \frac{\nu}{\mu+\nu}, \frac{\mu+2\nu}{\mu+\nu}, -\frac{a_0 e^{t(\mu+\nu)}}{a_1}\right]\right)}{a_1\nu}\right)^{-2+\Delta}}{\frac{\rho_{m0}}{(a_0 e^{t\mu} + a_1 e^{-t\nu})^3} + c\left(\frac{e^{-t\nu}\left(a_1 + a_0 e^{t(\mu+\nu)}\right)\left(a_1 C_1 \nu - e^{t\nu} {}_2F_1\left[1, \frac{\nu}{\mu+\nu}, \frac{\mu+2\nu}{\mu+\nu}, -\frac{a_0 e^{t(\mu+\nu)}}{a_1}\right]\right)}{a_1\nu}\right)^{-2+\Delta}}$$

(64)

Therefore, from Eq. (64), we can found $\epsilon_2 = \frac{\dot{\epsilon_1}}{H\epsilon_1}$, ratio of the amplitude of tensor perturbations (primordial gravitational waves) to the amplitude of scalar perturbations $r = 16\epsilon_1$, and spectral index $n_s = 1 - 2\epsilon_1 - 2\epsilon_2$.

selecting the bounce field potential $V(\phi)$. Using exponential functions, the potential can also be selected to provide an attractor solution in the expanding and contracting branches of the cosmological evolution.
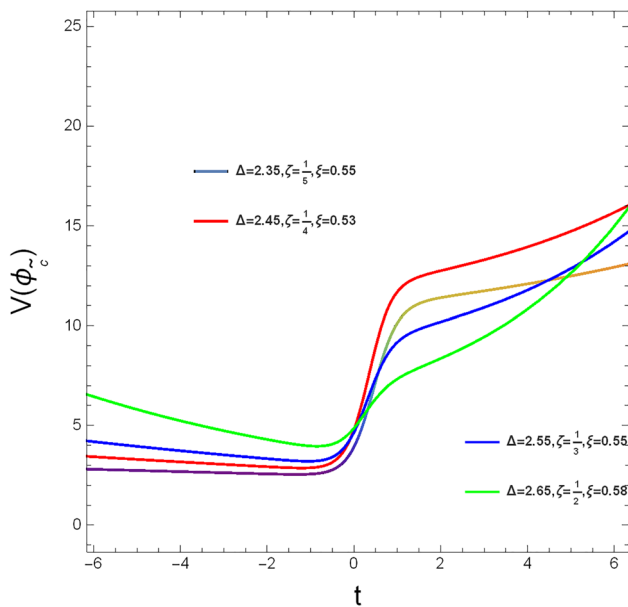
Fig. 33 Evolution of reconstructed canonical potential $V(\phi_{\tilde{c}})$ in viscous non-interacting bouncing scenario
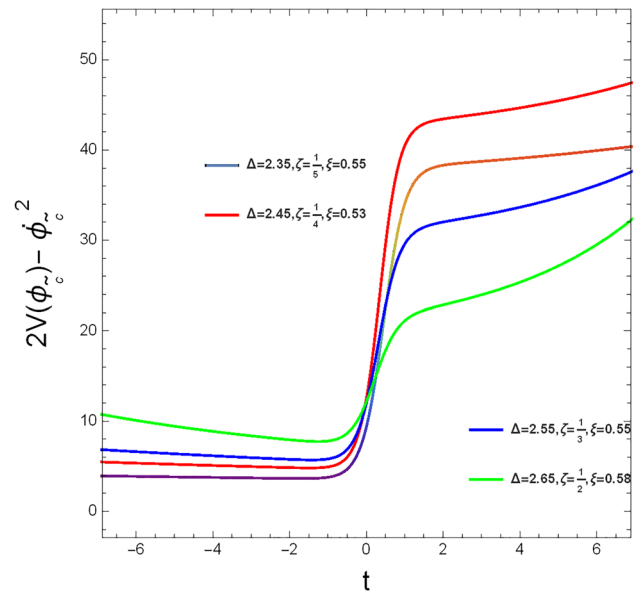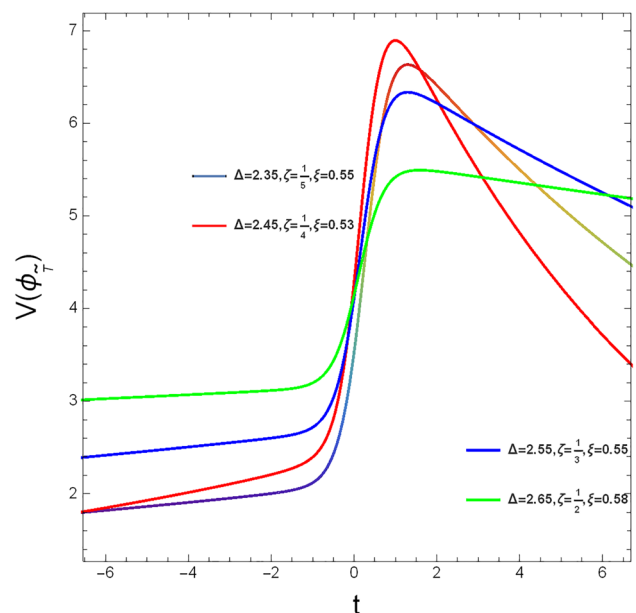

Fig. 34 Evolution of reconstructed $2V - \dot{\phi}_{\tilde{c}}^2$ in viscous non-interacting bouncing canonical scalar field scenario

(e) Cosmological dynamics of canonical scalar field in bouncing universe

Substituting ρ_{BHDE} and w_{BHDE} in Eq. (57) by ρ_{Total} and w_{eff} of bouncing viscous non-interacting scenario from Eqs. (37) and (40), we get the bounce field potential $V(\phi)$ in canonical scalar field case. Here, we have plotted, a bounce field potential which violates the Null Energy Condition for a brief period, inducing the bounce, and $2V - \dot{\phi}_{\tilde{c}}^2$ in Figs. 33 and 34 respectively. The generated potential function from the canonical scalar field is shown against time t in Fig. 33. To understand how the potential varies with the parameter, several trajectories are generated for various Δ values. The figure makes it evident that the potential rises with time t. This result is consistent with the observations. As we study $2V - \dot{\phi}_{\tilde{c}}^2$, we observe that it is positive (see Fig. 34) with respect to t. Nonetheless, $2V - \dot{\phi}_{\tilde{c}}^2$ is almost flat near the time increase, even though it begins to rise sharply; for this reason, we can regard it as consistent.

(f) Cosmological dynamics of tachyonic scalar field in bouncing universe

Moving on, we introduce a second field $V(\phi_{\tilde{T}})$ to represent an arbitrary tachyonic potential that satisfies the Null Energy Condition and $\phi_{\tilde{T}}$ be the matter field. For an understanding of the cosmic acceleration with bouncing scale factor, observed through Big Bounce and BHDE background fluid, the tachyonic scalar field is of particular interest. By substituting ρ_{Total} and w_{eff} of the bouncing viscous non-interacting scenario from Eq. (37) with ρ_{BHDE} and w_{BHDE} in Eqs. (61, 62) and the effective EoS parameter, we obtain tachyonic potential $V(\phi_{\tilde{T}})$ and in Figs. 35 and 36, we have

Fig. 35 Evolution of reconstructed tachyon potential $V(\phi_{\tilde{T}})$ in viscous non-interacting bouncing scenario

plotted $V(\phi_{\tilde{T}})$ and $2V - \dot{\phi}_{\tilde{T}}^2$ in relation to time respectively. Plotting the constructed potential function from the tachyonic scalar field against the time under the viscous BHDE as background fluid is shown in Fig. 35. At the background level the universe is homogenous, and thus both the bounce field potential $V(\phi_{\tilde{T}})$ and the matter field $\phi_{\tilde{T}}$ are only functions of cosmic time. Figure 36 plots $2V - \dot{\phi}_{\tilde{T}}^2$ against time; this corresponds with the observational data, which indicates that $2V >> \dot{\phi}_{\tilde{T}}^2$.
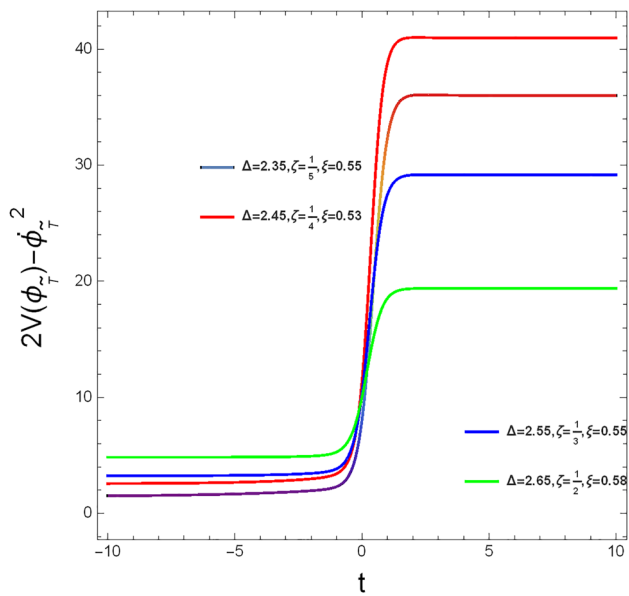
Fig. 36 Evolution of reconstructed $2V - \dot{\phi}_{\tilde{T}}^2$ in viscous non-interacting intermediate tachyon scalar field scenario

5 Thermodynamic implications to barrow holographic dark energy

Following the clarification of the black hole's thermodynamical characteristics [120,154,155], it has been said that the black hole's entropy is proportionate to the horizon's area A which is

$$S = \frac{A}{4G}, \ where, \ A = 4\pi r_H^2 \qquad (65)$$

There have been extensive and current studies where the relation between gravity and thermodynamics has been explained. This is known as the Bekenstein–Hawking entropy, where r_H is the horizon radius and we operate in units where $h = k_B = c = 1$ [156,157]. Using the cosmological apparent horizon [158] as a realisation of the thermodynamics of space-time [156], we have found in the studies that the FRW equations can also be viewed as the first law of thermodynamics when we take into account the Bekenstein–Hawking entropy. More precisely, [72] provides the Barrow entropy.We know our $BHDE$ parameter is Δ, and A_0 is a constant in the equation mentioned above.

5.1 Thermodynamics of interacting BHDE

In this section, we derive the rate of change of the total entropy and then examine the validity of generalized second law of thermodynamics. It is widely accepted that the thermodynamical characteristics of a black hole apply equally to a cosmic horizon, and thus thermodynamical study of the gravity theory is an intriguing area of research. Furthermore, when the universe is restricted by an apparent horizon, the

first Friedmann equation in the FRW universe may also be used to determine the first law of thermodynamics, which holds in a black hole horizon. Bekenstein [120] postulated in 1973 that there is a relationship between a black hole's thermodynamics and event of horizon, meaning that the black hole's event of horizon is a measure of its entropy. This concept has been expanded to include cosmological model horizons, such that each horizon is equivalent to an entropy. Consequently, the second law of thermodynamics was modified such that, in its generalized form, the total of all horizon-related time derivatives of entropies plus the time derivative of normal entropy must be positive, meaning that the total of entropies must increase with time. This gives good reason to use the future event horizon as the cosmic horizon for analysing any cosmological model's thermodynamic features. In light of the aforementioned justifications, we have regarded the universe as a thermodynamic system here, enclosed by the cosmic event horizon of radius [159,166]. The future event horizon is that the distance that light travels from the present time to infinity, is defined by

$$R_E = a(t) \int_t^\infty \frac{dt}{a(t)} \ \ and \ \ \dot{R}_E = H R_E - 1 \qquad (66)$$

where, $a(t)$ denotes scale factor.

Let us consider S_f and S_h are the entropy of the fluid and the entropy of the horizon containing the fluid, therefore, the total entropy (S) will be $S = S_h + S_f$. Like any isolated macroscopic system, S needs to satisfy the following relations that are consistent with the rules of thermodynamics,

$$\dot{S} = \frac{dS}{dt} \geq 0 \ \ and \ \ \ddot{S} = \frac{d^2S}{dt^2} < 0. \qquad (67)$$

It is important to take into account that the inequality $\dot{S} \geq 0$ and $\ddot{S} \leq 0$ are referred to, respectively, as the generalised second law (GSL) [157–165] of thermodynamics and thermodynamic equilibrium (TE), in this context. In addition, the GSL ought to hold true throughout the entirety of the universe's history, whereas the TE ought to hold during the latter stages of that evolution. Here, we have considered, both viscous BHDE and dark matter in interacting scenario to check validity of GSL. When evaluating the validity of GSL, we use the assumption that the future event horizon and the dark sectors are in equilibrium, which means that the temperature of the horizon is the same for both dark energy and dark matter. Because of their interaction, there will inevitably be a temperature equilibrium between the dark sections. The horizon and the dark regions will shortly reach equilibrium. Consequently, the temperatures of each component in the universe will eventually converge to the horizon temperature. The temperature of the event horizon be

$$T_E = \frac{1}{2\pi R_E} \qquad (68)$$

As previously mentioned, we considered the BHDE and DM as the components in the energy budget, then we can write

$$S_f = S_{BHDE} + S_{DM} \tag{69}$$

where, S_{BHDE} and S_{DM} represents the entropies of the coupled fluid of BHDE and DM respectively and here, T is considered as the temperature of this coupled fluid inside the horizon. As a result, for the individual matter contents, the first law of thermodynamics ($TdS = dE + PdV$) can be expressed as follows:

$$TdS_{BHDE} = dE_{BHDE} + P_{BHDE}dV, \tag{70}$$

$$TdS_{DM} = dE_{DM} + P_{DM}dV = dE_{DM}, \tag{71}$$

where the horizon volume is expressed as $V = \frac{4}{3}\pi R_E{}^3$. Again, $E_{BHDE} = \frac{4}{3}\pi R_E{}^3 \rho_{BHDE}$ and $E_{DM} = \frac{4}{3}\pi R_E{}^3 \rho_{DM}$ represents the internal energies of BHDE and pressure-less DM. Therefore, by differentiating Eqs. (70) and (71), we can get $\dot{S}_{BHDE}$ and $\dot{S}_{DM}$ respectively. Finally, it is imperative to note that in this particular context, the fluid temperature T must match the event horizon temperture T_E; otherwise, the energy flow would cause this geometry to deform. Therefore, the entropy inside this coupled BHDE and DM will be:

$$\dot{S}_f = \dot{S}_{BHDE} + \dot{S}_{DM} \tag{72}$$

Again, entropy of the horizon can be defined as:

$$S_E = \frac{A_0}{4G} \frac{A}{A_0}^{(1+\Delta)}, \text{ where, } A = 4\pi R_E^3 \tag{73}$$

Here, $A = 4\pi R_E^3$ and R_E are the surface area and the radius of the future event horizon. Therefore, by differentiating Eq. (72), we can arrive at the expression:

$$S = \dot{S}_E + \dot{S}_f = \dot{S}_E + \dot{S}_{BHDE} + \dot{S}_{DM} \tag{74}$$

Hence, by replacing R_E from Eq. (15), $\rho_m\, from$ Eq. (26), ρ_{Total} and P of viscous interacting emergent BHDE in Eqs. 72, 73, 74, we can get the time derivative of total entropy in emergent interacting scenario and it is plotted in Fig. 37. Figure 37 is consistent with the time derivative of total entropy as it satisfies the inequality $\dot{S} \geq 0$. Thermal equilibrium is also established in this case also for $\ddot{S} \leq 0$.

We can obtain the time derivative of total entropy in intermediate interacting scenario by substituting R_E from Eq. (27), $\rho_m\, from$ Eq. (32), ρ_{Total}, and P of viscous interacting emergent BHDE in Eqs. (72), (73), (74). Since Fig. 38 satisfies the inequality $\dot{S} \geq 0$, it is consistent with the time derivative of total entropy. In this instance, thermal equilibrium is also established for $\ddot{S} \leq 0$.

Specifically, we present for the first time a non-singular generalized entropy. The non-singular behavior of the proposed entropy function can be helpfully described in the context of bouncing scenarios, where the universe experiences $H = 0$ at the moment of bounce. This section will discuss
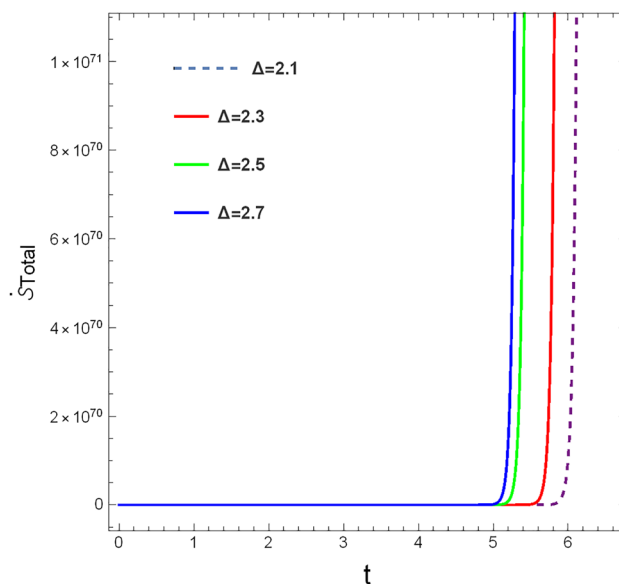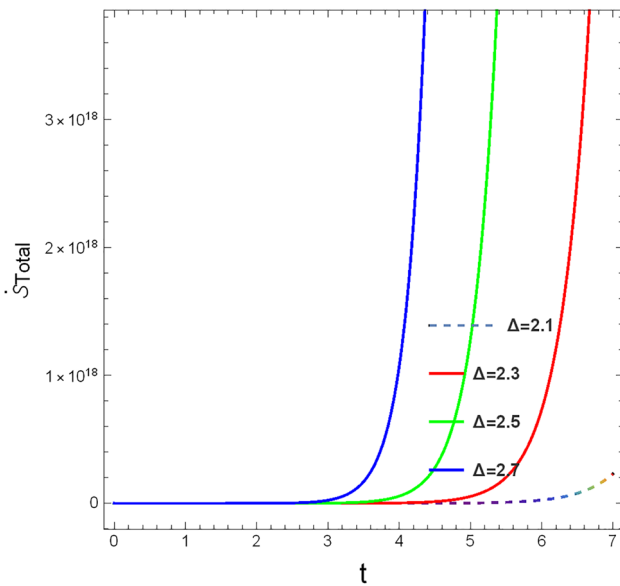

Fig. 37 The time derivative of the total entropy for future event horizon R_E using the first law of thermodynamics in the emergent interacting BHDE scenario

how the generalized entropy affects non-singular bounce cosmology. Specifically, we will look into whether an early universe bounce that is consistent with observational constraints can be generated by the entropic energy density. Here, we can establish the time derivative of total entropy in bouncing interacting scenario by substituting R_E from Eq. (34), $\rho_m\, from$ Eq. (41), ρ_{Total}, and P of viscous interacting emergent BHDE in Eqs. (72), (73), (74). Figure 39 satisfies the inequality $\dot{S} \geq 0$ in post bounce scenario, which is compatible. Although, in pre-bounce scenario, $S \to 0$

6 Conclusion

Singularity problem has been affecting inflation theories despite their remarkable achievements. Phenomenologically, one can avoid the singularity by taking into account that a non-singular bounce occurs prior to inflation. The bounce suggests that the universe may have been contracting from a large volume before our universe began to expand. In addition to offering a scientific explanation for the mysterious question of what our Universe looked like before inflation, the bounce scenario may also introduce some new elements into the early stages of our Universe and make predictions that may be found in later observations. In [96,97], the phenomenology of the bounce inflation scenario was first examined. It was demonstrated that, in addition to producing scale-invariant scalar perturbations that fit the data, such a scenario can also result in tilted spectrum, which can explain the suppression of the CMB TT spectrum at large scales. The perturbations generated prior to the bounce. Although conformal

Fig. 38 The time derivative of the total entropy for future event horizon R_E using the first law of thermodynamics in the intermediate interacting BHDE scenario
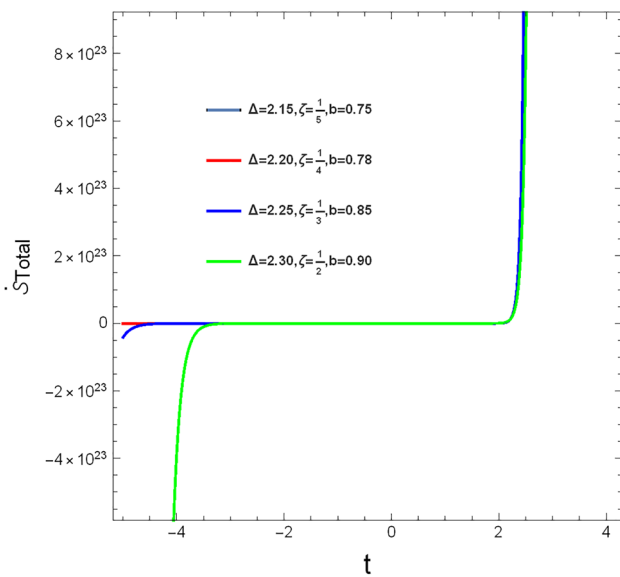
Fig. 39 The time derivative of the total entropy for future event horizon R_E using the first law of thermodynamics in the bouncing interacting BHDE scenario

transformation effectively addresses the majority of problems associated with the bouncing paradigm, it is important to note that certain problems may still arise as a result of the same transformation.

Our goal in this work was to establish a link between the singularities of the Big Bang and the Big Bounce, which can be solved generically without requiring the introduction of the non-standard kinetic operators needed for the effective field approach. The cosmological dynamics of a canonical

scalar field with an ekpyrotic like potential is also examined in this paper. Barrow holographic dark energy (BHDE) is formulated using dimensional analysis and the Barrow holographic principle. It should be noted that the BHDE differs significantly from the standard dark energy (DE) models in which the dark energy density is derived from a suitable scalar field or from one or more higher curvature terms in the Lagrangian. This is because the BHDE is based on the holographic principle rather than adding a term to the Lagrangian. The particle horizon (R_p) or the future event horizon (R_E) are typically used to calculate the horizon distance. Here, we have considered viscous BHDE as background fluid in interacting and non-interacting scenario for evolution of the universe, where the Barrow exponent lies in $(0, \infty)$. The purpose of the study [1] was to investigate if there is a form of the LIR that is appropriate enough to be considered equivalent to the generalized HDE in terms of the Barrow entropic dark energy model. In that case, the authors have examined the question: what is the equivalent LIR's form that corresponds to the entropic DE model of Barrow? Inspired by this [1] study, we have chosen the relaxed Barrow exponent that varies in accordance with the universe's cosmological expansion.

Cosmic expansion is significantly influenced by dissipative processes such as bulk viscosity, shear viscosity, and heat transport. When a cosmological fluid expands (or contracts) too quickly, it can cause the system to lose its local thermodynamic equilibrium and thus develop bulk viscosity. For this reason, we have studied emergent, intermediate and bouncing cosmology with respect to viscous BHDE in interacting and non-interacting scenario. In an emergent universe, single BHDE performs a vital role in the realization of inflation by taking the Big Bang singularity as the initial singularity. In Figs. 2, 3, we have plotted the expression of the effective EoS parameter w_{eff} and the deceleration parameter q respectively. w_{eff} behaves phantom rigorously, and q shows an accelerating emergent BHDE universe in a non-interacting scenario. Figure 4 shows our model is stable against small perturbations. Although, in Fig. 5, we have observed quintessence evolution of the universe by choosing interacting viscous BHDE scenario with the interaction term $Q = 3Hb^2\rho_m$. Figure 6 shows us the effective EoS parameter crosses the phantom boundary in a coupled fluid model similar to a single fluid model of the BHDE viscous emergent universe. Then, in the non-interacting intermediate scenario, we have plotted the effective EoS parameter ($w_{eff} = \frac{P+\Pi}{\rho_{Total}}$) in Fig. 7. The phantom scenario of effective EoS parameter and the reconstructed w_{eff} are unable to escape the big-rip by leaving the phantom, as shown in Fig. 7. The universe's accelerating expansion is shown in Fig. 8, and Fig. 9 demonstrates that our model is stable against small perturbations for all values of Δ. We have plotted viscous interacting BHDE in an intermediate scenario in Figs. 10 and 11. In Fig. 10, the

EoS parameter exhibits its quintessential behavior, while in Fig. 11, the effective EoS parameter is steadily approaching the phantom border. In the next subsection, we will address the cosmological field equations that correspond to the non-singular viscous bouncing scenario with the BHDE single fluid model for background evolution. In Fig. 1, we have seen the bouncing evolution of the universe with bouncing point $H_B = 0$. Furthermore, we presented the EoS parameter, effective EoS parameter, and total energy density (ρ_{Total}) in Figs. 12, 13, and 14, respectively, for the non-interacting bouncing scenario. Fig. 12 shows the proper chronological growth of the universe. In Fig. 12, the BHDE energy density rises in the post-bounce scenario, increases in the pre-bounce scenario due to expansion, and reaches its minimum value at $t = 0$ during the bounce. The EoS parameter crosses the phantom border in both the pre- and post-bounce scenarios, as shown in Fig. 13. As shown in Fig. 14, the reconstructed w_{eff}, effective EoS parameter is behaving quintessence in the pre-bounce scenario and phantom in the post-bounce scenario. In the post-bounce scenario, the phantom scenario of the effective EoS parameter is able to escape the big-rip. Figure 15 shows the accelerating expansion of the universe, and Fig. 16 shows that, for all values of Δ in both pre and post bounce scenarios, our model is stable against small perturbations. As illustrated in Fig. 17, the growth of the reconstructed EoS parameter (left panel) diverges due to viscous BHDE in an interacting scenario. The EoS parameter behaves as quintessence in the pre-bounce case and crosses the phantom boundary in the post-bounce instance. The effective EoS parameter prevents the Big Rip singularity in the post-bounce scenario (right panel). It is clear that as we increase the interaction coefficient b, both EoS parameters are strictly moving to phantom.

In literature, the holographic principle is frequently applied to late time acceleration. We have used the principle in the early time inflationary scenario here, having been inspired by this. The energy density is proportional to the inverse of length squared, according to the principle. The energy density produced should be sufficient to drive the inflation since it is anticipated that the length scale will be extremely small during the inflation. Since the entropy is the known source of holographic dark energy, changing the entropy law can change the nature of the DE. Here, we've examined one such modification using the Barrow entropy relation, which was inspired by the COVID-19 virus's shape. It was discovered that the structure of a black hole had intricate fractal features brought about by these quantum corrections. Using $\Delta > 0$, we have investigated an inflationary scenario characterized by a universe full of Barrow holographic dark energy. In emergent, intermediate, and non-singular bouncing scenarios, a number of analytical solutions for the model were discovered, including the slow-roll parameters, scalar spectral index, and tensor-to-scalar ratio. Lastly, a pos-

sible correspondence between scalar fields and the BHDE is investigated. For this, the Tachyonic field and the canonical scalar field are both employed. Plotting the potential produced by the two distinct fields allows one to see how it has evolved. The trend can be observed to be in line with the observational data. This work demonstrates that BHDE may be a prime contender to power the universe's early inflationary scenario. In Figs. 19, 21 we have established inflationary scenarios in viscous emergent and intermediate BHDE universe and nice exit from inflation with Big Bang singularity. Figure 20 is consistent with Planck2018 dataset in emergent case although Fig. 22 is inconsistent with Planck2018 dataset in intermediate case. In Figs. 23, 25 we can see canonical scalar field is realised in emergent and intermediate viscous BHDE scenario. The distinctive quality of tachyon fields-their imaginary mass and negative kinetic energy-is captured in Figs. 27, 29 respectively.

In this paper, we have shown that in models with both canonical and non-canonical scalar fields, stable bouncing cosmologies are generic and straightforward to achieve. Without departing from the weak-gravity regime, we have built models that can stably realize a transition from contraction to expansion by Fig. 31 in a flat Friedmann universe. The evolution must be free of gradient instabilities and the perturbations must stay ghost-free for the bounce to be considered healthy. To be more precise, we have deduced a set of sufficient conditions on the bounce inflation theory's form to ensure the stability of the evolution at the turnaround point. As we've demonstrated, it's easy to realize fast inflation in a post-bounce scenario in Fig. 32. However, we have not been able to create a model in which the entire history of expansion-including the distant past and distant future-is under control. The model presented here avoids the cosmic singularity problem and is geodesically complete, as is the case with most non-singular bouncing cosmologies. In the BHDE non-interacting viscous scenario, this double exponential bouncing scale factor can realize the canonical and non-canonical scalar field (see Figs. 33, 35). Additionally, as the universe contracts prior to the bounce, the current patch comes into causal contact, and we offer a solution to the horizon problem that does not require inflation. We will explicitly calculate the horizon size to explain how bouncing cosmologies and the model considered in this paper solve the horizon problem. The main goal is, as mentioned earlier, to find out if the time derivative of the total entropy of the universe, bounded by the horizons and the normal entropy, stays at nonnegative level. We have thought of the universe surrounded by event horizon in order to accomplish the same. We have already incorporated event horizon to find out the density of BHDE. The type of time derivative of the total entropy for the event horizon has been studied for the emergent, intermediate, and non-singular bouncing interacting viscous BHDE scenarios. The generalized second law is applicable to all

emergent, intermediate, and post-bounce scenarios, regardless of the curvature of the universe, as we can observe from Figs. 37, 38, 39 when the model parameters are chosen appropriately.

In summary, the Barrow entropic dark energy model is found to be equivalent to the generalized HDE, with the corresponding cut-off determined in terms of future event horizon. As we wrap up, let's discuss the current study's findings in light of the very recent research by [167], whose authors suggested the holographic realisation of a cosmic scenario from constant roll inflation (early on) to the dark energy era (later on), with an intermediate radiation-dominated era followed by a Kamionkowski-like reheating stage. We suggest expanding our research to include phases that actually follow the inflationary phase in light of [167], which will show how early inflation and late time acceleration are unified.

Data availability   This manuscript has no associated data or the data will not be deposited. [Authors' comment: This is a theoretical study and no experimental data is associated with the manuscript.]

Code Availability   The manuscript has no associated code/software. [Authors' comment:Code/Software sharing not applicable to this article as no code/softwarewas generated or analysed during the current study.]

Declarations

Conflict of interest   The authors state that none of their known competing financial interests or personal connections could have had an impact on the work that came out in this paper.

Funded by SCOAP³.

References

1. S. Nojiri, S.D. Odintsov, T. Paul, Barrow entropic dark energy: a member of generalized holographic dark energy family. Phys. Lett. B **825**, 136844 (2022)

2. S. Nojiri, S.D. Odintsov, T. Paul, Different faces of generalized holographic dark energy. Symmetry **13**(6), 928 (2021)

3. S. Perlmutter et al., Discovery of a supernova explosion at half the age of the Universe. Nature **391**(6662), 51–54 (1998)

4. S. Perlmutter et al., Measurements of Ω and λ from 42 high-redshift supernovae. Astrophys. J. **517**(2), 565 (1999)

5. B.P. Schmidt et al., The high-Z supernova search: measuring cosmic deceleration and global curvature of the universe using type Ia supernovae. Astrophys. J. **507**(1), 46 (1998)

6. D.J. Hillier, D.L. Miller, Constraints on the evolution of massive stars through spectral analysis. I. The WC5 Star HD 165763. Astrophys. J. **519**(1), 354 (1999)

7. B. Boisseau et al., Reconstruction of a scalar-tensor theory of gravity in an accelerating universe. Phys. Rev. Lett. **85**(11), 2236 (2000)

8. C.L. Bennett et al., First-year Wilkinson microwave anisotropy probe (WMAP)* observations: foreground emission. Astrophys. J. Suppl. Ser. **148**(1), 97 (2003)

9. D.N. Spergel et al., First-year Wilkinson Microwave Anisotropy Probe (WMAP)* observations: determination of cosmological parameters. Astrophys. J. Suppl. Ser. **148**(1), 175 (2003)

10. N. Jarosik et al., Seven-year Wilkinson microwave anisotropy probe (WMAP*) observations: sky maps, systematic errors, and basic results. Astrophys. J. Suppl. Ser. **192**(2), 14 (2011)

11. G. Hinshaw et al., Nine-year Wilkinson Microwave Anisotropy Probe (WMAP) observations: cosmological parameter results. Astrophys. J. Suppl. Ser. **208**(2), 19 (2013)

12. N.A. Bahcall et al., The cosmic triangle: revealing the state of the universe. Science **284**(5419), 1481–1488 (1999)

13. M. Tegmark et al., Cosmological parameters from SDSS and WMAP. Phys. Rev. D **69**(10), 103501 (2004)

14. L. Amendola, S. Tsujikawa, *Dark Energy: Theory and Observations* (Cambridge University Press, Cambridge, 2010)

15. Planck Collaboration et al., Planck 2013 results. XVI. Cosmological parameters. AA **571**, A16 (2014)

16. T. Padmanabhan, Dark energy: mystery of the millennium. AIP Conference Proceedings, vol. 861. no. 1 (American Institute of Physics, 2006)

17. T. Padmanabhan, T. Roy Choudhury, A theoretician's analysis of the supernova data and the limitations in determining the nature of dark energy. Mon. Not. R. Astron. Soc. **344**(3), 823–834 (2003)

18. E.J. Copeland, M. Sami, S. Tsujikawa, Dynamics of dark energy. Int. J. Mod. Phys. D **15**(11), 1753–1935 (2006)

19. V. Sahni, A. Starobinsky, Reconstructing dark energy. Int. J. Mod. Phys. D **15**(12), 2105–2132 (2006)

20. S.M. Carroll, The cosmological constant. Living Rev. Relativ. **4**(1), 1–56 (2001)

21. T. Padmanabhan, Cosmological constant-the weight of the vacuum. Phys. Rep. **380**(5–6), 235–320 (2003)

22. J.-P. Wu, D.-Z. Ma, Y. Ling, Quintessence reconstruction of the new agegraphic dark energy model. Phys. Lett. B **663**(3), 152–159 (2008)

23. Y.-F. Cai et al., Quintom cosmology: theoretical implications and observations. Phys. Rep. **493**(1), 1–60 (2010)

24. P.J. Steinhardt, A quintessential introduction to dark energy. Philos. Trans. R. Soc. Lond. Ser. A Math. Phys. Eng. Sci. **361**(1812), 2497–2513 (2003)

25. S. Nojiri, S.D. Odintsov, S. Tsujikawa, Properties of singularities in the (phantom) dark energy universe. Phys. Rev. D **71**(6), 063004 (2005)

26. S. Nojiri, S.D. Odintsov, Unifying phantom inflation with late-time acceleration: scalar phantom-non-phantom transition model and generalized holographic dark energy. Gen. Relativ. Gravit. **38**, 1285–1304 (2006)

27. S. Nojiri, S.D. Odintsov, Effective equation of state and energy conditions in phantom/tachyon inflationary cosmology perturbed by quantum effects. Phys. Lett. B **571**(1–2), 1–10 (2003)

28. E. Elizalde et al., Dark energy: vacuum fluctuations, the effective phantom phase, and holography. Phys. Rev. D **71**(10), 103504 (2005)

29. Z.-K. Guo et al., Cosmological evolution of a quintom model of dark energy. Phys. Lett. B **608**(3–4), 177–182 (2005)

30. Y.-F. Cai et al., Bouncing universe with quintom matter. J. High Energy Phys. **2007**(10), 071 (2007)

31. G.-B. Zhao et al., Perturbations of the quintom models of dark energy and the effects on observations. Phys. Rev. D **72**(12), 123515 (2005)

32. B. Feng et al., Oscillating quintom and the recurrent universe. Phys. Lett. B **634**(2–3), 101–105 (2006)

33. J.S. Bagla, H.K. Jassal, T. Padmanabhan, Cosmology with tachyon field as dark energy. Phys. Rev. D **67**(6), 063504 (2003)

34. M.R. Setare, J. Sadeghi, A.R. Amani, Interacting tachyon dark energy in non-flat universe. Phys. Lett. B **673**(4–5), 241–246 (2009)

35. E.J. Copeland et al., What is needed of a tachyon if it is to be the dark energy? Phys. Rev. D **71**(4), 043003 (2005)

36. C. Bonvin, C. Caprini, R. Durrer, No-go theorem for k-essence dark energy. Phys. Rev. Lett. **97**(8), 081303 (2006)

37. C. Armendariz-Picon, E.A. Lim, Haloes of k-essence. J. Cosmol. Astropart. Phys. **2005**(08), 007 (2005)

38. N. Bose, A.S. Majumdar, K-essence model of inflation, dark matter, and dark energy. Phys. Rev. D **79**(10), 103517 (2009)

39. V. Gorini, A. Kamenshchik, U. Moschella, Can the Chaplygin gas be a plausible model for dark energy? Phys. Rev. D **67**(6), 063509 (2003)

40. N. Bilić, G.B. Tupper, R.D. Viollier, Unification of dark matter and dark energy: the inhomogeneous Chaplygin gas. Phys. Lett. B **535**(1–4), 17–21 (2002)

41. M.C. Bento, O. Bertolami, A.A. Sen, Generalized Chaplygin gas, accelerated expansion, and dark-energy-matter unification. Phys. Rev. D **66**(4), 043507 (2002)

42. R. Bean, O. Dore, Are Chaplygin gases serious contenders for the dark energy? Phys. Rev. D **68**(2), 023515 (2003)

43. X. Zhang, Statefinder diagnostic for holographic dark energy model. Int. J. Mod. Phys. D **14**(09), 1597–1606 (2005)

44. Y. Gong, Extended holographic dark energy. Phys. Rev. D **70**(6), 064029 (2004)

45. Q.-G. Huang, M. Li, The holographic dark energy in a non-flat universe. J. Cosmol. Astropart. Phys. **2004**(08), 013 (2004)

46. K. Bamba et al., Dark energy cosmology: the equivalent description via different theoretical models and cosmography tests. Astrophys. Space Sci. **342**, 155–228 (2012)

47. G.'T Hooft, Dimensional reduction in quantum gravity (1993). arXiv preprint arxiv:gr-qc/9310026

48. L. Susskind, The world as a hologram. J. Math. Phys. **36**(11), 6377–6396 (1995)

49. R. Bousso, The holographic principle. Rev. Mod. Phys. **74**(3), 825 (2002)

50. L. Susskind, Entanglement and chaos in de Sitter holography: an SYK example (2021). arXiv preprint arXiv:2109.14104

51. A.G. Cohen, D.B. Kaplan, A.E. Nelson, Effective field theory, black holes, and the cosmological constant. Phys. Rev. Lett. **82**(25), 4971 (1999)

52. S. Del Campo, J.C. Fabris, R. Herrera, W. Zimdahl, Holographic dark-energy models. Phys. Rev. D **83**(12), 123006 (2011)

53. W. Zimdahl, D. Pavón, Interacting holographic dark energy. Class. Quantum Gravity **24**(22), 5461 (2007)

54. Y.S. Myung, Holographic principle and dark energy. Phys. Lett. B **610**(1–2), 18–22 (2005)

55. C. Gao et al., Holographic dark energy model from Ricci scalar curvature. Phys. Rev. D **79**(4), 043511 (2009)

56. E.N. Saridakis, Restoring holographic dark energy in brane cosmology. Phys. Lett. B **660**(3), 138–143 (2008)

57. M.R. Setare, E.N. Saridakis, Correspondence between holographic and Gauss–Bonnet dark energy models. Phys. Lett. B **670**(1), 1–4 (2008)

58. E.N. Saridakis, Holographic dark energy in braneworld models with a Gauss–Bonnet term in the bulk. Interacting behavior and the $w = -1$ crossing. Phys. Lett. B **661**(5), 335–341 (2008)

59. M. Jamil, E.N. Saridakis, M.R. Setare, Holographic dark energy with varying gravitational constant. Phys. Lett. B **679**(3), 172–176 (2009)

60. M.R. Setare, E.N. Saridakis, Non-minimally coupled canonical, phantom and quintom models of holographic dark energy. Phys. Lett. B **671**(3), 331–338 (2009)

61. A. Pasqua, S. Chattopadhyay, R. Myrzakulov, Power-law entropy-corrected holographic dark energy in Hořava–Lifshitz cosmology with Granda–Oliveros cut-off. Eur. Phys. J. Plus **131**, 1–51 (2016)

62. B. Pourhassan et al., Holographic dark energy from fluid/gravity duality constraint by cosmological observations. Phys. Dark Universe **20**, 41–48 (2018)

63. S. Nojiri, S.D. Odintsov, Unifying phantom inflation with late-time acceleration: scalar phantom-non-phantom transition model and generalized holographic dark energy. Gen. Relativ. Gravit. **38**, 1285–1304 (2006)

64. E. Elizalde et al., Dark energy: vacuum fluctuations, the effective phantom phase, and holography. Phys. Rev. D **71**(10), 103504 (2005)

65. M. Khurshudyan, On a holographic dark energy model with a Nojiri–Odintsov cut-off in general relativity. Astrophys. Space Sci. **361**, 1–12 (2016)

66. C. Feng et al., Testing the viability of the interacting holographic dark energy model by using combined observational constraints. J. Cosmol. Astropart. Phys. **2007**(09), 005 (2007)

67. S. Wang, Y. Wang, M. Li, Holographic dark energy. Phys. Rep. **696**, 1–57 (2017)

68. X. Zhang, W. Feng-Quan, Constraints on holographic dark energy from the latest supernovae, galaxy clustering, and cosmic microwave background anisotropy observations. Phys. Rev. D **76**(2), 023502 (2007)

69. M.-M. Zhao et al., Search for sterile neutrinos in holographic dark energy cosmology: reconciling Planck observation with the local measurement of the Hubble constant. Phys. Rev. D **96**(4), 043520 (2017)

70. Y.-Z. Ma, Y. Gong, X. Chen, Features of holographic dark energy under combined cosmological constraints. Eur. Phys. J. C **60**, 303–315 (2009)

71. G.G. Luciano, Y. Liu, Lagrangian reconstruction of Barrow holographic dark energy in interacting tachyon model. Symmetry **15**(5), 1129 (2023)

72. J.D. Barrow, The area of a rough black hole. Phys. Lett. B **808**, 135643 (2020)

73. C. Tsallis, Possible generalization of Boltzmann–Gibbs statistics. J. Stat. Phys. **52**, 479–487 (1988)

74. S. Carlip, Logarithmic corrections to black hole entropy, from the Cardy formula. Class. Quantum Gravity **17**(20), 4175 (2000)

75. S. Nojiri, S.D. Odintsov, T. Paul, Towards a smooth unification from an ekpyrotic bounce to the dark energy era. Phys. Dark Universe **35**, 100984 (2022)

76. Y.-F. Cai, Exploring bouncing cosmologies with cosmological surveys. Sci. China Phys. Mech. Astron. **57**, 1414–1430 (2014)

77. Y.-F. Cai, D.A. Easson, R. Brandenberger, Towards a nonsingular bouncing cosmology. J. Cosmol. Astropart. Phys. **2012**(08), 020 (2012)

78. E.I. Buchbinder, J. Khoury, B.A. Ovrut, New ekpyrotic cosmology. Phys. Rev. D **76**(12), 123503 (2007)

79. S. Saha, S. Chattopadhyay, Realization of bounce in a modified gravity framework and information theoretic approach to the bouncing point. Universe **9**(3), 136 (2023)

80. S. Saha, E. Güdekli, S. Chattopadhyay, A study on the various aspects of bounce realisation for some choices of scale factors. Symmetry **15**(7), 1332 (2023)

81. A.A. Starobinsky, Ya.B. Zel'Dovich, The spontaneous creation of the Universe. Sov. Sci. Rev. Sect., 103–144 (1988)

82. A.H. Guth, Inflationary universe: a possible solution to the horizon and flatness problems. Phys. Rev. D **23**(2), 347 (1981)

83. S. Capozziello, S'I. Nojiri, S.D. Odintsov, Unified phantom cosmology: inflation, dark energy and dark matter under the same standard. Phys. Lett. B **632**(5–6), 597–604 (2006)

84. A.R. Liddle, L. Arturo Ureña-López, Inflation, dark matter, and dark energy in the string landscape. Phys. Rev. Lett. **97**(16), 161301 (2006)

85. I.P. Neupane, B.M.N. Carter, Towards inflation and dark energy cosmologies from modified Gauss–Bonnet theory. J. Cosmol. Astropart. Phys. **2006**(06), 004 (2006)

86. S. Panda, M. Sami, S. Tsujikawa, Inflation and dark energy arising from geometrical tachyons. Phys. Rev. D **73**(2), 023515 (2006)

87. V.K. Oikonomou, Unifying inflation with early and late dark energy epochs in axion F(R) gravity. Phys. Rev. D **103**(4), 044036 (2021)

88. J.D. Barrow, A. Paliathanasis, Reconstructions of the dark-energy equation of state and the inflationary potential. Gen. Relativ. Gravit. **50**, 1–25 (2018)

89. S.W. Hawking, R. Penrose, The singularities of gravitational collapse and cosmology. Proc. R. Soc. Lond. A Math. Phys. Sci. **314**(1519), 529–548 (1970)

90. S.W. Hawking, G.F.R. Ellis, *The Large Scale Structure of Space-Time* (Cambridge University Press, Cambridge, 2023)

91. A. Borde, A. Vilenkin, Eternal inflation and the initial singularity. Phys. Rev. Lett. **72**(21), 3305 (1994)

92. H.-H. Xiong, T. Qiu, Y.-F. Cai, X. Zhang, Cyclic universe with quintom matter in loop quantum cosmology. Mod. Phys. Lett. A **24**, 1237 (2009). [arXiv:0711.4469]

93. H.-H. Xiong et al., Oscillating universe with quintom matter. Phys. Lett. B **666**(3), 212–217 (2008)

94. Y.-S. Piao, Can the universe experience many cycles with different vacua? Phys. Rev. D **70**(10), 101302 (2004)

95. Y.-S. Piao, Proliferation in cycle. Phys. Lett. B **677**(1–2), 1–5 (2009)

96. Y.-S. Piao, B. Feng, X. Zhang, Suppressing the CMB quadrupole with a bounce from the contracting phase to inflation. Phys. Rev. D **69**(10), 103520 (2004)

97. Y.-S. Piao, S. Tsujikawa, Z. Xinmin, Inflation in string-inspired cosmology and suppression of CMB low multipoles. Class. Quantum Gravity **21**(18), 4455 (2004)

98. A.R. Liddle, P. Parsons, J.D. Barrow, Formalizing the slow-roll approximation in inflation. Phys. Rev. D **50**(12), 7222 (1994)

99. Z. Yi, Y. Gong, On the constant-roll inflation. J. Cosmol. Astropart. Phys. **2018**(03), 052 (2018)

100. G. Calcagni, Slow-roll parameters in braneworld cosmologies. Phys. Rev. D **69**(10), 103508 (2004)

101. S.M. Leach, A.R. Liddle, Constraining slow-roll inflation with WMAP and 2dF. Phys. Rev. D **68**(12), 123508 (2003)

102. J. Martin, H. Motohashi, T. Suyama, Ultra slow-roll inflation and the non-Gaussianity consistency relation. Phys. Rev. D **87**(2), 023514 (2013)

103. H.V. Peiris, R. Easther, Recovering the inflationary potential and primordial power spectrum with a slow roll prior: methodology and application to wmap three year data. J. Cosmol. Astropart. Phys. **2006**(07), 002 (2006)

104. M. Gasperini, G. Veneziano, The pre-big bang scenario in string cosmology. Phys. Rep. **373**(1–2), 1–212 (2003)

105. J.E. Lidsey, D. Wands, E.J. Copeland, Superstring cosmology. Phys. Rep. **337**(4–5), 343–492 (2000)

106. Z.-G. Liu, Z.-K. Guo, Y.-S. Piao, Obtaining the CMB anomalies with a bounce from the contracting phase to inflation. Phys. Rev. D **88**(6), 063539 (2013)

107. Y.-S. Piao, Design of a cyclic multiverse. Phys. Lett. B **691**(5), 225–229 (2010)

108. J.-L. Lehners, P.J. Steinhardt, Planck 2013 results support the cyclic universe. Phys. Rev. D **87**(12), 123533 (2013)

109. V. Sahni, A. Toporensky, Cosmological hysteresis and the cyclic universe. Phys. Rev. D **85**(12), 123542 (2012)

110. S.I. Nojiri, S.D. Odintsov, V.K. Oikonomou, T. Paul, Unifying holographic inflation with holographic dark energy: a covariant approach. Phys. Rev. D **102**(2), 023540 (2020)

111. S.I. Nojiri, S.D. Odintsov, E.N. Saridakis, Holographic bounce. Nucl. Phys. B **949**, 114790 (2019)

112. S.I. Nojiri, S.D. Odintsov, E.N. Saridakis, Holographic inflation. Phys. Lett. B **797**, 134829 (2019)

113. T. Qiu, Y.-T. Wang, G-bounce inflation: towards nonsingular inflation cosmology with Galileon field. J. High Energy Phys. **2015**(4), 1–28 (2015)

114. Ö. Güngör, G.D. Starkman, A classical, non-singular, bouncing universe. J. Cosmol. Astropart. Phys. **2021**(04), 003 (2021)

115. Y.-F. Cai et al., Bouncing cosmologies with dark matter and dark energy. Universe **3**(1), 1 (2016)

116. J. de Haro, Y.-F. Cai, An extended matter bounce scenario: current status and challenges. Gen. Relativ. Gravit. **47**, 1–24 (2015)

117. C. Eckart, The thermodynamics of irreversible processes. III. Relativistic theory of the simple fluid. Phys. Rev. **58**(10), 919 (1940)

118. L.D. Landau, E.M. Lifshitz, *Fluid Mechanics* (Butterworth, Oxford, 1987)

119. W. Israel, J.M. Stewart, Thermodynamics of nonstationary and transient effects in a relativistic gas. Phys. Lett. A **58**(4), 213–215 (1976)

120. J.D. Bekenstein, Black holes and entropy. Phys. Rev. D **7**(8), 2333 (1973)

121. P.C.W. Davies, Cosmological horizons and the generalised second law of thermodynamics. Class. Quantum Gravity **4**(6), L225 (1987)

122. S. Wang, Y. Wang, M. Li, Holographic dark energy. Phys. Rep. **696**, 1–57 (2017)

123. M. Li, A model of holographic dark energy. Phys. Lett. B **603**(1–2), 1–5 (2004)

124. J.D. Barrow, The deflationary universe: an instability of the de Sitter universe. Phys. Lett. B **180**(4), 335–339 (1986)

125. J.D. Barrow, String-driven inflationary and deflationary cosmological models. Nucl. Phys. B **310**(3–4), 743–763 (1988)

126. G.L. Murphy, Big-bang model without singularities. Phys. Rev. D **8**(12), 4231 (1973)

127. X.-H. Meng, X. Dou, Singularities and entropy in bulk viscosity dark energy model. Commun. Theor. Phys. **56**(5), 957 (2011)

128. R.H. Brandenberger, The matter bounce alternative to inflationary cosmology (2012). arXiv preprint arXiv:1206.4196

129. R. Brandenberger, P. Peter, Bouncing cosmologies: progress and problems. Found. Phys. **47**, 797–850 (2017)

130. J. de Haro, Y.-F. Cai, An extended matter bounce scenario: current status and challenges. Gen. Relativ. Gravit. **47**, 1–24 (2015)

131. T. Padmanabhan, Emergent perspective of gravity and dark energy. Res. Astron. Astrophys. **12**(8), 891 (2012)

132. A. Jawad, A. Pasqua, S. Chattopadhyay, Holographic reconstruction of f(G) gravity for scale factors pertaining to emergent, logamediate and intermediate scenarios. Eur. Phys. J. Plus **128**, 1–9 (2013)

133. U. Debnath, S. Chattopadhyay, M. Jamil, Fractional action cosmology: some dark energy models in emergent, logamediate, and intermediate scenarios of the universe. J. Theor. Appl. Phys. **7**, 1–19 (2013)

134. S. Cao et al., Ultra-compact structure in intermediate-luminosity radio quasars: building a sample of standard cosmological rulers and improving the dark energy constraints up to z 3. Astron. Astrophys. **606**, A15 (2017)

135. K. Bamba et al., Bouncing cosmology in modified Gauss–Bonnet gravity. Phys. Lett. B **732**, 349–355 (2014)

136. M.S. Berman, F.M. Gomide, Cosmological models with constant deceleration parameter. Gen. Relativ. Gravit. **20**, 191–198 (1988)

137. Y. Gong, A. Wang, Reconstruction of the deceleration parameter and the equation of state of dark energy. Phys. Rev. D **75**(4), 043520 (2007)

138. A. Jawad, S. Chattopadhyay, Cosmological analysis of models via pilgrim dark energy. Astrophys. Space Sci. **357**(1), 37 (2015)

139. S. Saha, S. Chattopadhyay, Viscous generalised Chaplygin Gas under the purview of f (T) gravity and the model assessment through probabilistic information theory. Phys. Scr. **97**(4), 045006 (2022)

140. D. Pavón, B. Wang, Le Châtelier–Braun principle in cosmological physics. Gen. Relativ. Gravit. **41**, 1–5 (2009)

141. D. Nandi, Bounce from inflation. Phys. Lett. B **809**, 135695 (2020)

142. Sh. Nojiri, S.D. Odintsov, V.K. Oikonomou, Modified gravity theories on a nutshell: inflation, bounce and late-time evolution. Phys. Rep. **692**, 1–104 (2017)

143. D.I. Kaiser, Primordial spectral indices from generalized Einstein theories. Phys. Rev. D **52**(8), 4295 (1995)

144. M. Sasaki, E.D. Stewart, A general analytic formula for the spectral index of the density perturbations produced during inflation. Prog. Theor. Phys. **95**(1), 71–78 (1996)

145. J. Martin, C. Ringeval, V. Vennin, Encyclopædia inflationaris. Phys. Dark Universe **5**, 75–235 (2014)

146. R.P. Woodard, Perturbative quantum gravity comes of age. Int. J. Mod. Phys. D **23**(09), 1430020 (2014)

147. M. Li, C. Lin, Y. Wang, Some issues concerning holographic dark energy. J. Cosmol. Astropart. Phys. **2008**(05), 023 (2008)

148. K. Bamba et al., Dark energy cosmology: the equivalent description via different theoretical models and cosmography tests. Astrophys. Space Sci. **342**, 155–228 (2012)

149. A. Mohammadi et al., Tsallis holographic dark energy for inflation. Phys. Rev. D **103**(8), 083505 (2021)

150. A. Sen, Tachyon matter. J. High Energy Phys. **2002**(07), 065 (2002)

151. V.A. Belinskii, I.M. Khalatnikov, E.M. Lifshitz, Oscillatory approach to a singular point in the relativistic cosmology. Adv. Phys. **19**(80), 525–573 (1970)

152. J.K. Erickson et al., Kasner and mixmaster behavior in universes with equation of state w> 1. Phys. Rev. D **69**(6), 063514 (2004)

153. Y.-F. Cai, D.A. Easson, R. Brandenberger, Towards a nonsingular bouncing cosmology. J. Cosmol. Astropart. Phys. **2012**(08), 020 (2012)

154. E.N. Saridakis, S. Basilakos, The generalized second law of thermodynamics with Barrow entropy. Eur. Phys. J. C **81**(7), 644 (2021)

155. S.W. Hawking, Particle creation by black holes. Commun. Math. Phys. **43**(3), 199–220 (1975)

156. T. Jacobson, Thermodynamics of spacetime: the Einstein equation of state. Phys. Rev. Lett. **75**(7), 1260 (1995)

157. T. Padmanabhan, Gravity and the thermodynamics of horizons. Phys. Rep. **406**(2), 49–125 (2005)

158. R.-G. Cai, S.P. Kim, First law of thermodynamics and Friedmann equations of Friedmann–Robertson–Walker universe. J. High Energy Phys. **2005**(02), 050 (2005)

159. D. Bak, S.-J. Rey, Cosmic holography+. Class. Quantum Gravity **17**(15), L83 (2000)

160. K. Karami, A. Abdolmaleki, Generalized second law of thermodynamics in f (T) gravity. J. Cosmol. Astropart. Phys. **04**, 007 (2012)

161. A.V. Frolov, L. Kofman, Inflation and de Sitter thermodynamics. J. Cosmol. Astropart. Phys. **2003**(05), 009 (2003)

162. K. Karami et al., Thermodynamics of apparent horizon in modified FRW universe with power-law corrected entropy. J. High Energy Phys. **2011**(8), 1–14 (2011)

163. K. Karami, S. Ghaffari, M.M. Soltanzadeh, The generalized second law of gravitational thermodynamics on the apparent and event horizons in FRW cosmology. Class. Quantum Gravity **27**(20), 205021 (2010)

164. A. Abdolmaleki, T. Najafi, K. Karami, Generalized second law of thermodynamics in scalar-tensor gravity. Phys. Rev. D **89**(10), 104041 (2014)

165. M.R. Setare, S. Shafei, A holographic model of dark energy and the thermodynamics of a non-flat accelerated expanding universe. J. Cosmol. Astropart. Phys. **2006**(09), 011 (2006)

166. K. Bamba et al., Generalized second law of thermodynamics in f (T) gravity with entropy corrections. Astrophys. Space Sci. **344**, 259–267 (2013)

167. S.I. Nojiri, S.D. Odintsov, T. Paul, Holographic realization of constant roll inflation and dark energy: An unified scenario. Phys. Lett. B **841**, 137926 (2023)